

**REPUBLIC OF LEBANON
COUNCIL FOR DEVELOPMENT AND RECONSTRUCTION**

**ASSESSMENT OF SITE-SPECIFIC EARTHQUAKE HAZARD
FOR BISRI DAM, LEBANON**

Prepared by:
M. Erdik, K. Şeşetyan, M.B. Demircioğlu, E. Harmandar

Boğaziçi University
Kandilli Observatory and Earthquake Research Institute
Department of Earthquake Engineering

October, 2014

LIST OF CONTENTS

1. INTRODUCTION.....	3
2. EARTHQUAKE RESISTANT DESIGN CRITERIA: DESIGN BASIS GROUND MOTION.....	4
3. NEO-TECTONICS	6
4. SEISMICITY	14
5. GROUND MOTION PREDICTION EQUATIONS	21
6. PROBABILISTIC SEISMIC HAZARD ANALYSIS.....	23
6.1. PREVIOUS STUDIES	23
6.2. THE PSHA MODEL USED IN THIS STUDY	23
7. VERTICAL RESPONSE SPECTRA FOR 144 YEAR RETURN PERIOD	26
8. DETERMINISTIC SEISMIC HAZARD.....	28
9. DIRECTIONALITY EFFECTS.....	31
10. NEAR FAULT EFFECTS	31
11. DESIGN BASIS RESPONSE SPECTRA	33
12. SPECTRUM COMPATIBLE HORIZONTAL GROUND MOTION	33
13. CONCLUSIONS.....	39
REFERENCES.....	39

1. INTRODUCTION

This report covers the assessment of the site specific earthquake hazard for Bisri Dam in Lebanon, the location of which is given in Figure 1.

The main physical ingredients of seismic hazard assessment are the tectonic setting of the region, the earthquake occurrences and the local site conditions. These regional physical features, the applicable ground motion prediction models and the appropriate stochastic model for probabilistic hazard analysis will be discussed in the following sections.

Earthquake hazard will be quantified using both probabilistic and deterministic approaches (PSHA and DSHA respectively) in accordance with the selected design criteria. The design basis earthquake ground motion will be quantified using the uniform hazard.

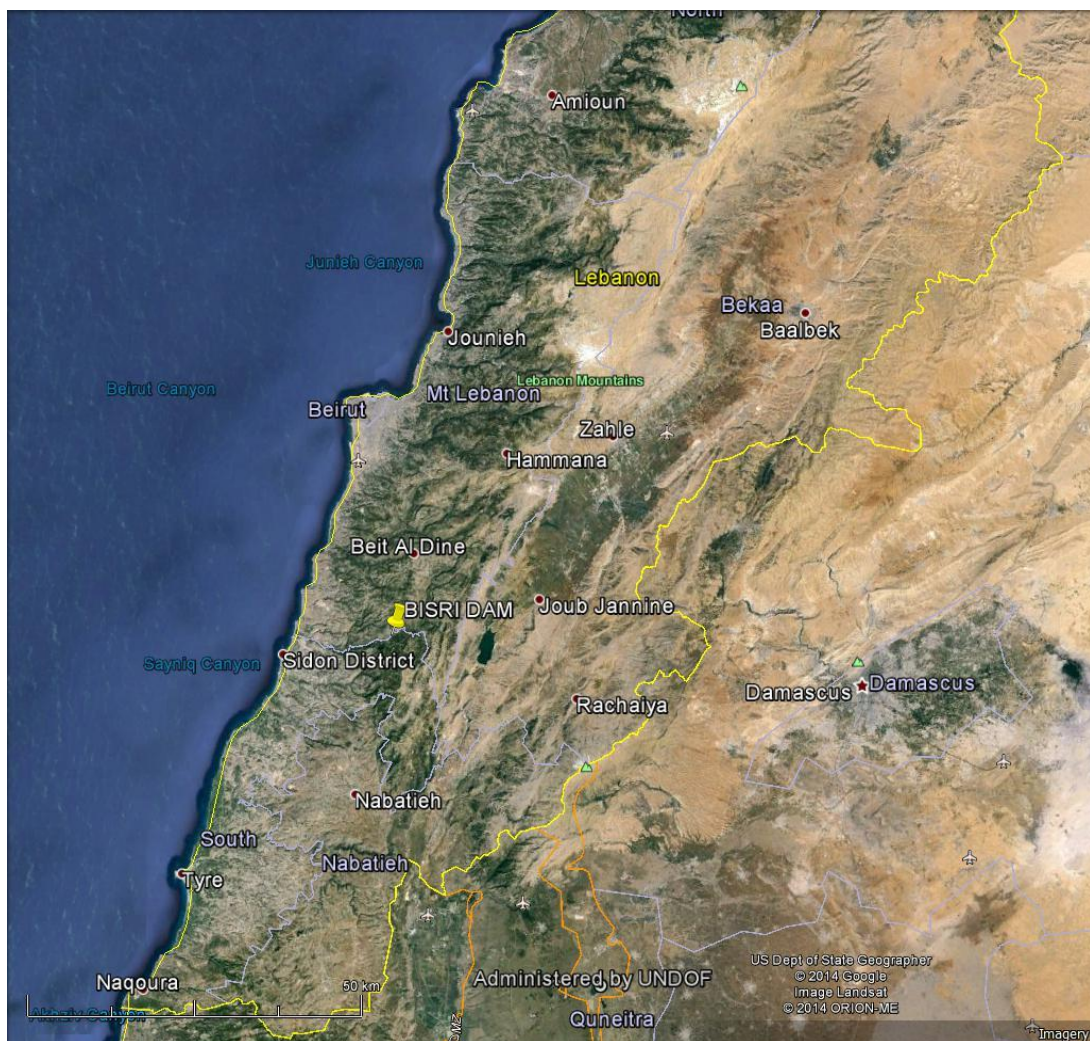


Figure 1. Location of Bisri Dam.

2. EARTHQUAKE RESISTANT DESIGN CRITERIA: DESIGN BASIS GROUND MOTION

The earthquake resistant design criteria prepared for the Bisri Dam (ECIDAH, 1997) essentially refers to the Operating Basis Earthquake (OBE), probabilistically associated with a return period of 144 years (USCOLD Criteria), and the Maximum Credible Earthquake (MCE), 84-percentile ground motion deterministically obtained from the MCE scenarios.

The deterministic OBE and MCE scenarios provided by ECIDAH (1997) are respectively M7.3 and M5.7 on Roum Fault both at 2km distance from the Bisri Dam. The Peak Ground Acceleration (PGA) for the MCE and OBE at the dam site were assessed to be respectively to be 0.7g and 0.52g, presumably for engineering bed-rock. The vertical ground motions were simply taken as 2/3 of the horizontal component.

Figure 2, taken from ECIDAH (1997) displays the 84-percentile spectrum specified for the MCE level design. This was specified to be the response spectra to be used for dynamic analysis of the embankment dam and for rigid structures which require the 5% damping ratio.

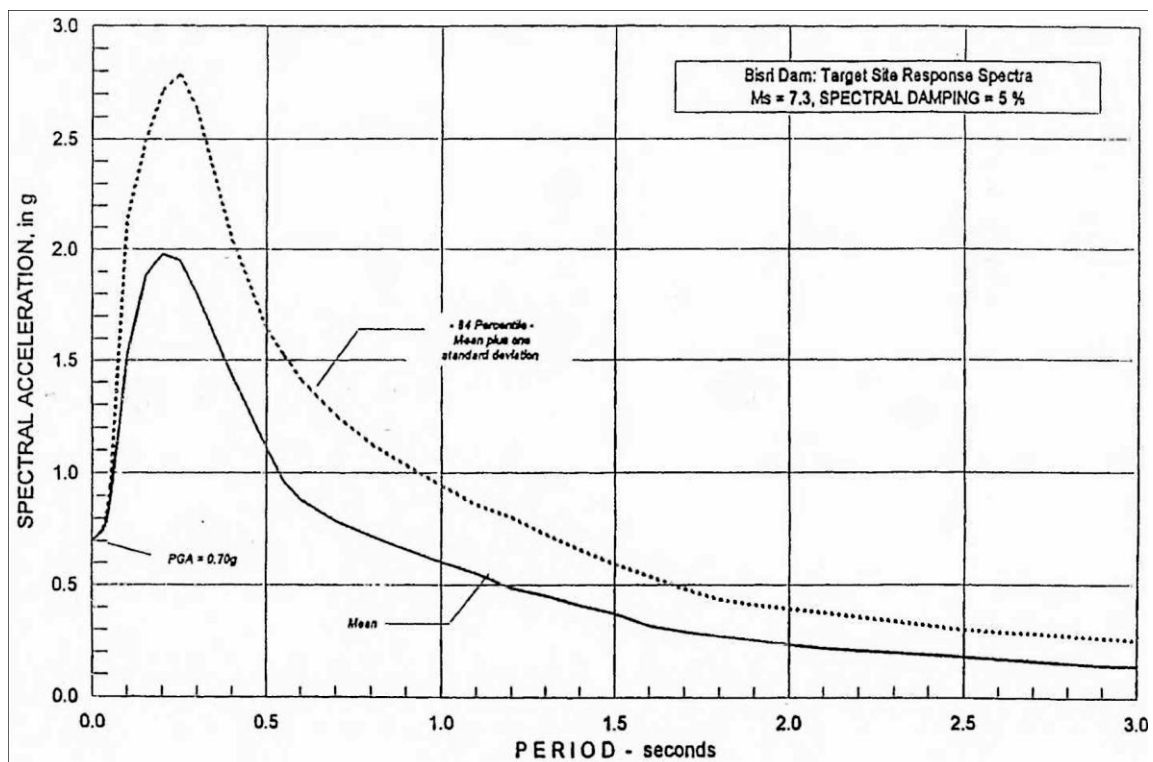


Figure 2. MCE target spectrum (ECIDAH, 1997).

Although, at the time of its computation it represented the state-of-the-art, today, the validity and rationality of this MCE response spectra, developed using the knowledge that dates back to 1976 (e.g. Seed at al., 1976), is highly questionable, since over the almost 40 year period, now we have both quantitatively and qualitatively much better earthquake strong motion data sets and consequently, much more reliable ground motion prediction expressions (GMPEs). Similarly, the frequency-independent, 2/3 ratio between vertical and horizontal motion considered in ECIDAH (1997) is now outdated, especially for near fault conditions.

Bard (2014), who has provided three sets of ground motion compatible with the MCE response spectra originally presented in ECIDAH (1997), has also stated that "*those which have been used in the reference documents are now quite old (1982) and look obsolete, compared to the huge wealth of high quality data recorded by the new networks deployed throughout the world*".

Under the Subsection 5.1 of the Dam Review Board (DRB) Report No.1 (November 2013), it has been requested to "Perform a seismic hazard study to define the characteristics of the earthquakes that may be encountered at the site (design basis ground motion levels)". Although there was no objection to the methodology used in the development of the three sets of spectrum compatible ground motion in Bard (2014), the Board has questioned the target spectra used in this process.

As such, the earthquake resistant design criteria need to be updated and the design basis response spectra associated with the SEE level ground motions need to be recomputed based on the current data, knowledge and state-of-the-art methodologies.

Current approach for the earthquake resistant design of the dams relies on the "performance based design" as documented in the guidelines of the Committee on Seismic Aspects of Dam Design of the International Commission on Large Dams (ICOLD, 2010). ICOLD guidelines call for a two level design based on the Operating Basis Earthquake (OBE) and the Safety Evaluation Earthquake (SEE) together with the associated performance objectives.

Operating Basis Earthquake (OBE)

ICOLD Guidelines (1989). "*The Operating Basis Earthquake (OBE) represents the level of ground motion at the dam site at which only minor damage is acceptable, the dam, appurtenant structures and equipment should remain functional and damage easily repairable from the recurrence of the earthquake not exceeding the OBE*".

FEMA (2005). "*The OBE is an earthquake that produces ground motions at the site that can reasonably be expected to occur within the service life of the project. The associated performance requirement is that the project functions with little or no damage, and without interruption of function. The purpose of the OBE is to protect against economic losses from damage or loss of service. Therefore, the return period may be based on economic considerations*".

USACE (1995, 2007): "*The OBE is an earthquake that can reasonably be expected to occur within the service life of the project, that is, with a 50% probability of exceedance during the service life (corresponding to a return period of 144 years for a project with a service life of 100 years). The OBE is determined by a PSHA.*"

Maximum Credible Earthquake (MCE)

ICOLD (1989, 2010). "*The MCE (Maximum Credible Earthquake) is the largest conceivable earthquake that appears possible along a recognized fault or within a geographically designated tectonic province, under the presently known or presumed tectonic framework*". ICOLD (2010), dropping the definition of MDE, further states that "*The most severe ground motion affecting a dam site due to an MCE scenario is referred to as the MCE ground motion*".

USACE (1995, 2007): *“This earthquake is defined as the greatest earthquake that can reasonably be expected to be generated by a specific source on the basis of seismological and geological evidence. Since a project site may be affected by earthquakes generated by various sources, each with its own fault mechanism, maximum earthquake magnitude, and distance from the site, multiple MCE’s may be defined for the site, each with characteristics ground motion parameters and spectral shape. The MCE is determined through a DSHA”*.

FEMA (2005). *“The MDE or Safety Evaluation Earthquake (SEE) is the earthquake that produces the maximum level of ground motions for which a structure is to be designed or evaluated. The MDE or SEE may be set equal to the MCE or to a design earthquake less than the MCE, depending on the circumstances”*.

ASCE 7-10 (2010): Uses the *“Maximum Considered Earthquake (MCE)”* to define the 2%/50 (2475 year average return period) earthquake ground motion, based on probabilistic methods. Deterministically it represents the ground motion that would result from the Maximum Credible Earthquake.

IAEA Safety Guide SSG-9 (2010) recommends both a PSHA and a DSHA be used for the assessment of the SL-2 (often denoted as a safe shutdown earthquake, SSE) level design basis ground motion, generally associated with a 10,000 year average return period. For DSHA implicitly a median-plus-one sigma hazard quantification is suggested to commensurate with the SL-2 level ground motion.

On the basis of these evaluations and considerations the following design basis ground motion levels can be decided:

The Operating Basis Earthquake will be determined as the probabilistically assessed earthquake ground motion for an average return period of 144 years. Under the action of this level of ground motion, the dam, appurtenant structures and equipment should remain functional and, if any, the minor damage should be easily repairable.

The Safety Evaluation Earthquake is the maximum level of ground motion for which the dam should be designed or analyzed. For the earthquake resistant design of the Bisri Dam the SEE level ground motion will be determined to correspond to the 84-percentile deterministic MCE (i.e. median plus one standard deviation). Under the SEE the stability of the dam and life safety must be ensured with no uncontrolled release of water from the reservoir.

3. NEO-TECTONICS

The Bisri Dam site is located in a region of complex tectonic plate interaction along the Dead Sea Transform Fault (DSTF), which is a 1000-kilometer-long left-lateral transform fault system that stretches between the Gulf of Aqaba, at the northern edge of the Red Sea, to the Taurus Mountains in southern Turkey. (Inset in Figure 3)

Daeron (2005), Gomez et.al (2007), Nemer and Meghraoui (2006) and Elias et al. (2007) provide studies of the tectonic features within Lebanon and vicinity. Essentially, DSTF can be divided into two main sections joined by a restraining bend along Lebanon. Within the Lebanese restraining bend, the DSTF splits into five main fault branches: the Roum, Yammouneh, Seghaya, Rachaiya and Hasbaya faults (Figure 3 through Figure 6).

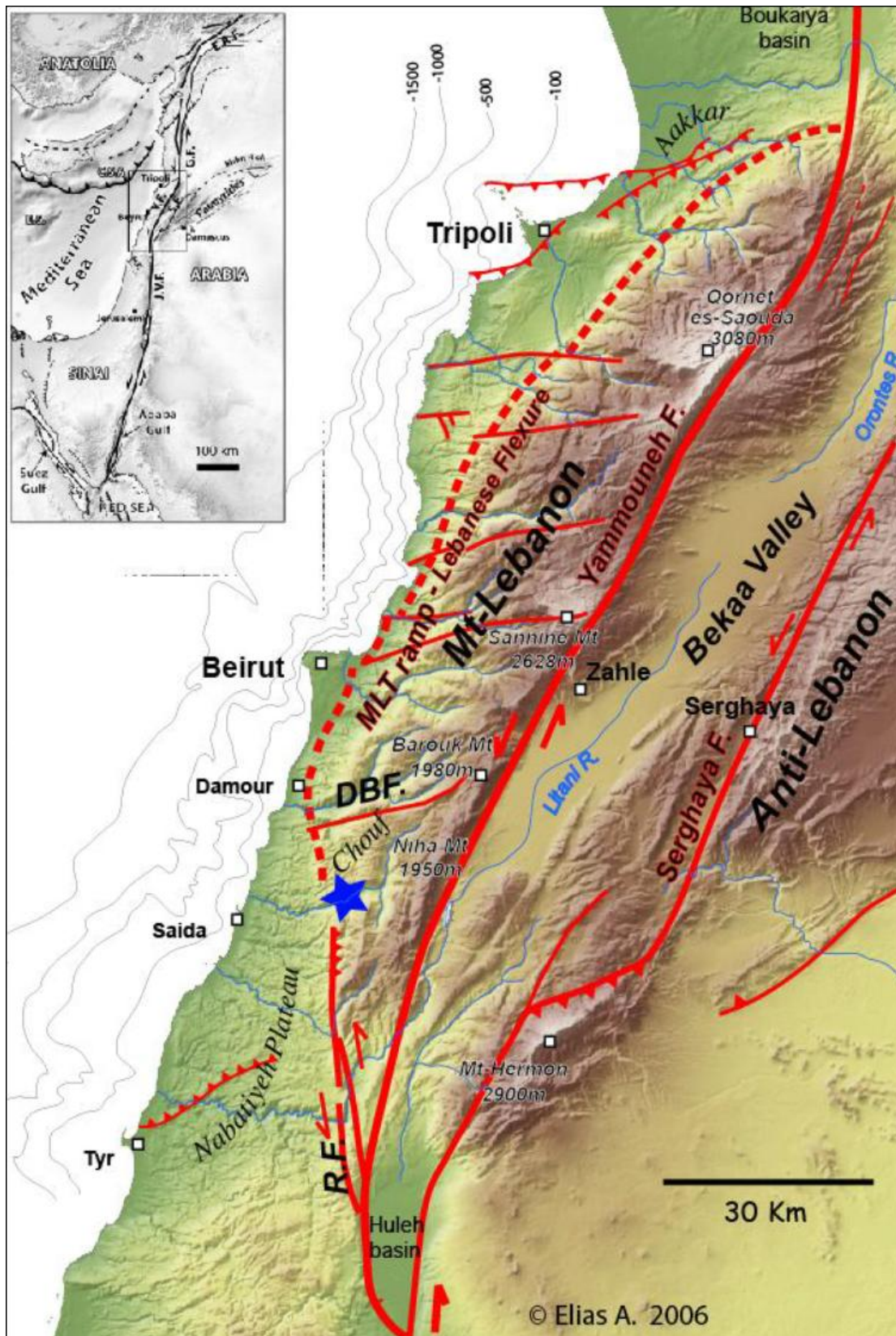


Figure 3. The Bisri Dam site (blue star) within the tectonic map of Lebanon. Red lines are for active faults. Dashed red line is for the blind Mount Lebanon Thrust ramp below the Lebanese Flexure as mapped on the surface. (R.F. = Roum Fault; DBF.= Damour Beiteddine Fault) (after Elias, 2014).

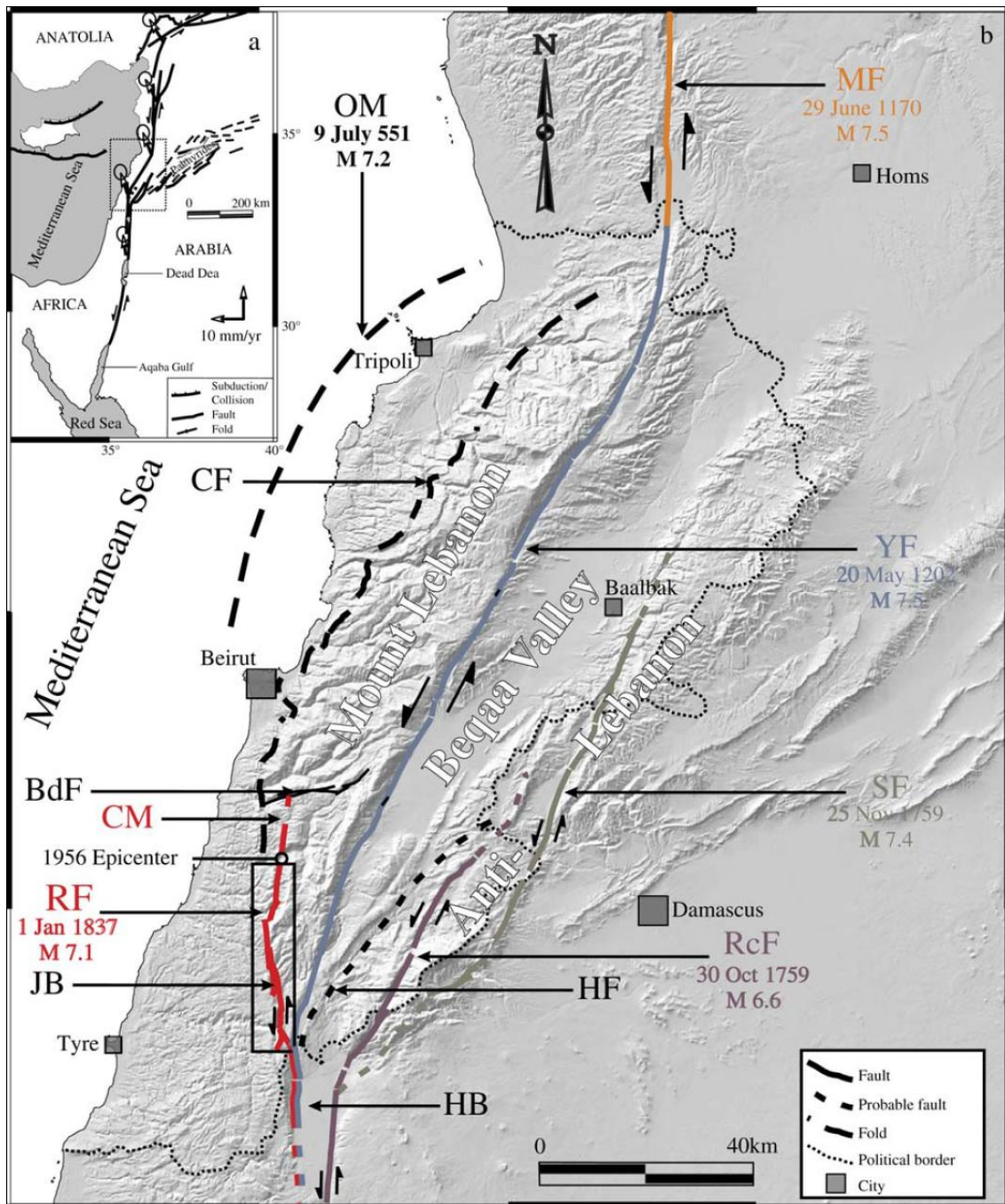


Figure 4. (a) The Dead Sea Transform Fault extending from the Gulf of Aqaba to southeast Turkey. It is a left-lateral transform fault with a general NeS trend except in Lebanon where it bends rightward to form a restraining bend. White arrows indicate the GPS velocities of the Arabian plate relative to adjacent plates. (b) Lebanese restraining bend showing the main units and structures: BdF, Beit-ed-Dine fault; CF, Coastal Flexure; CM, Chouf Monocline; HB, Hula basin; HF, Hasbaya fault; JB, Jarmaq basin; MF, Missyaf fault; OM, Offshore monocline; RcF, Rachaya fault; RF, Roush fault; SF, Serghaya fault; YF, Yammouneh fault. Note the epicentre location of the double-shock of the 1956 earthquake at the intersection between Roush fault and Chouf Monocline. Coloured faults are associated with large historical events (indicated by date and magnitude) that took place within the Lebanese restraining bend (after Nemer and Meghraoui, 2006).

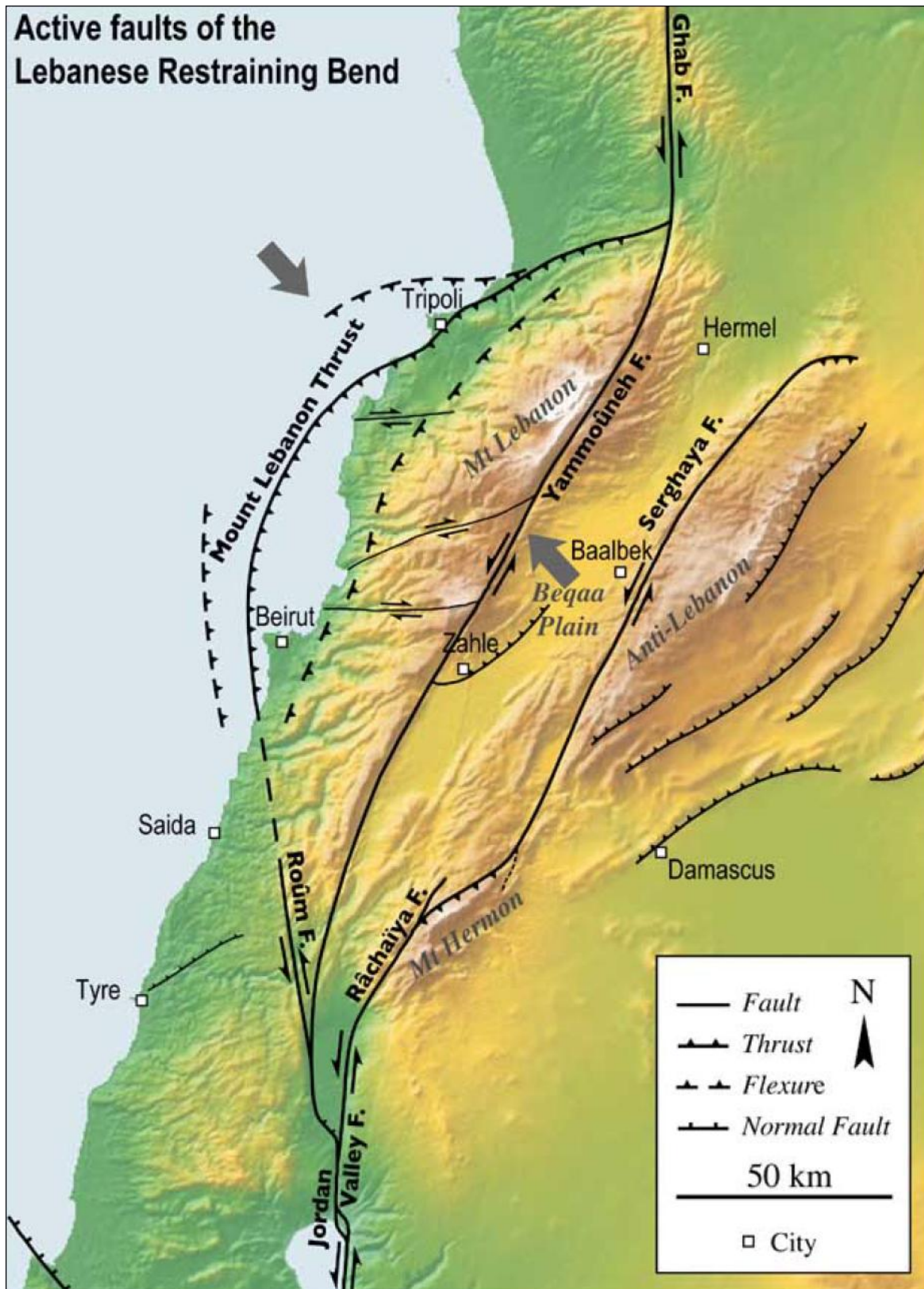


Figure 5. Map of the active faults in the Lebanese Restraining Bend (Daeron, 2005).

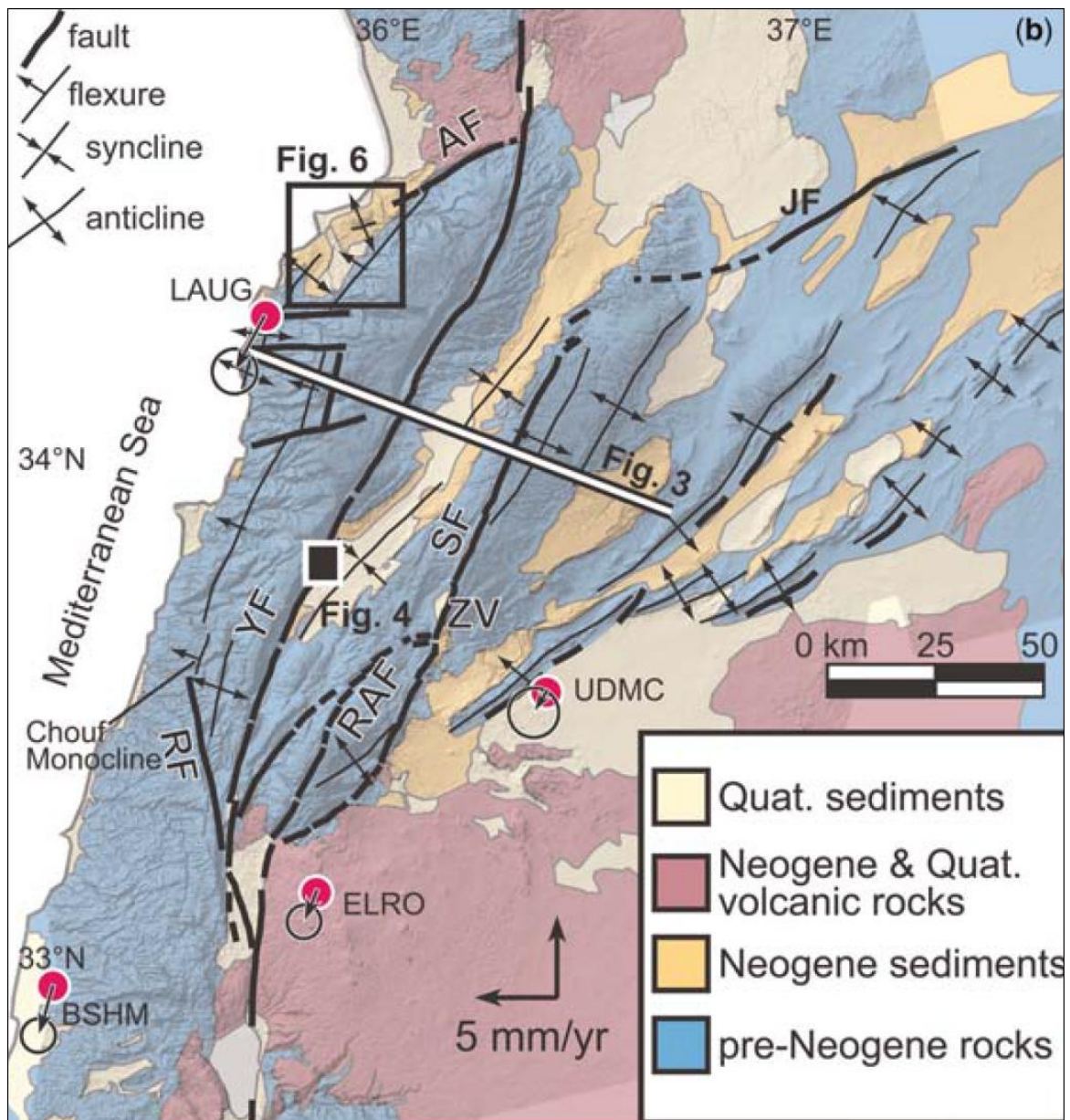


Figure 6. Map showing the general geology and the structure of the restraining bend. Arrows indicate velocities of continuous GPS sites (red circles) in an Arabia-fixed reference frame (Reilinger et al. 2006). Abbreviations: YF, Yammounh Fault, SF, Serghaya Fault; RF, Roucha Fault, RAF, Rachaya Fault; JF, Jhar Fault; HB, Hula Basin; MH $\frac{1}{4}$ Mount Hermon; TNP, Tyre–Nabatieh Plateau; and ZV, Zebadani Valley (After Gomez et al, 2007).

Elias (2014) provides a thorough description of the tectonic entities that would control the earthquake hazard at the Bisri Dam site.

The Yammounh Fault is an approximately 297-km-long, vertical strike-slip fault within the Lebanese restraining bend. The fault is active and has produced major earthquakes, the latest and strongest being M~7.6, 1202 event, with a coseismic slip of 5-6m (Daeron et al. 2007). The fault has a slip rate of 4-6mm/yr (Daeron et al. 2004, Gomez et al. 2007). The Yammounh Fault is at ~12km from the Dam site (Elias, 2014).

The Roucha Fault is a secondary branch of the Plate Boundary that splays into the Lebanon at Huleh south. It has a N-S strike over most of its 35km length. The fault is considered as mostly left-lateral strike-slip with a compressive component increasing towards the north. All

known geological mapping literature concur that the Roum Fault doesn't reach beyond the Awali river (the Dam site) as it merges into the Jezzine Anticline to the south. The Mazraa or Chouf Monocline to the north would correspond to its northern structural counterpart or equivalent (Dubertret 1955, Nemer & Meghraoui 2006, Elias et al. 2006). The Roum Fault has produced the two most recent destructive earthquakes onshore Lebanon the M~7, 1837 and the M~5.7, 1956 events. Its horizontal slip rate is ~1mm/yr.

Detailed mapping done by Nemer & Meghraoui (2006) indicated that the lineament of the Roum Fault is limited in extent to about 35 km from north of the Hula basin to the Awali river and that it disappears at ~ 33.67°N, where the fault bends northward and merges with the Chouf monocline. Nemer & Meghraoui (2006) further documented a northward decrease in the amount of deflection of major drainages across the Roum Fault. This was inferred to represent a northward decrease in strike-slip offset along the fault.

Similarly Gomez et al. (2007) states that the Roum fault lineament can be traced until approximately 33.84 N latitude. At the northern extent, the trace of the Roum Fault disappears as it bends northward and merges with the hinge of the Chouf monocline.

On the basis of the investigations done by Elias (2014) the mapped geological fault trace stops ~2km south of the Dam-site. Although the continuation of the fault further north into the Bisri valley was suggested by previous site investigations the site-specific studies and reassessment by Elias (2014) reveals no evidence of such continuation (Figure 7).

The Mount-Lebanon Thrust (MLT) ramp of the Lebanese Flexure is a crustal ramp that accommodates shortening associated with the Lebanese Restraining Bend of the Dead Sea Fault System. It is a shallow, east-dipping fault that offsets the seafloor offshore Lebanon and is connected at depth with the Yammouneh Fault. The surface expression of this blind ramp in the geology of the area is the Lebanese Flexure and associated folds. The Chouf or Mazraa flexure is part of this system. The MLT and the Flexure run along the entire Lebanese coast between Saida and Tripoli. A complex system of offshore thrust faults is also associated with the MLT (Figure 8a). The MLT and the This 40-45°, east-dipping thrust ramp mostly located in the upper, seismogenic, ~16km of the crust (Figure 8b) has a vertical slip-rate ~1.5 mm/yr (Elias et al. 2007). Evidence of rupture of the Quaternary and recent marine sediments at the tip of the MLT faults were observed during the SHALIMAR marine geophysical campaign (Elias et al. 2007, Carton et al. 2009). The location of the offshore ruptures and faults corresponds with the observed uplift of the shoreline as indicated by stairs of uplifted marine terraces (Elias et al. 2007).

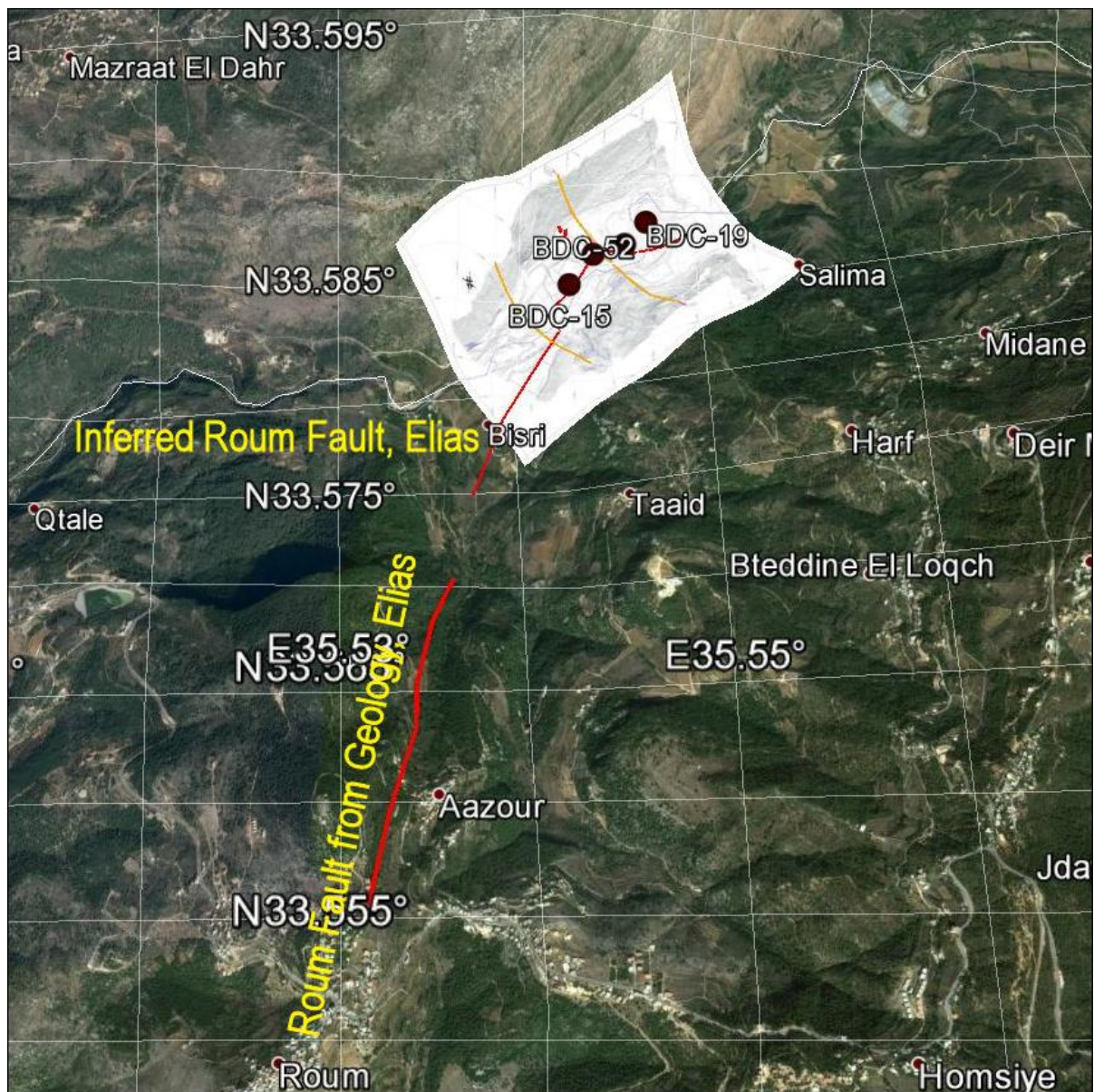


Figure 7. Location of the Rourm Fault to the south of the Bisri Dam site (After Elias, 2014).

The Bisri Dam site is located in the south of MLT ramp in the transfer area between the MLT and the Rourm Fault (Figure 8a). A geological cross-section of the area at the south end of the ramp helps constrain the geometry of the ramp at depth (Figure 8b).

The M~7.5, AD 551 earthquake is the best-known event associated with this fault system. It ruptured the entire ramp where possible co-seismic rupture between 2-3m was also inferred based on measured uplift indicators along the shoreline between Tripoli and Saida (Elias et. al, 2007). The surface rupture of this event was located in the offshore at the tip of the main ramp and further away on some of the smaller thrusts located in front of it (to the west). Based on the mapped fault trace, the expected MLT co-seismic rupture can therefore be at least 40km away from the Bisri Dam site (Elias, 2014).

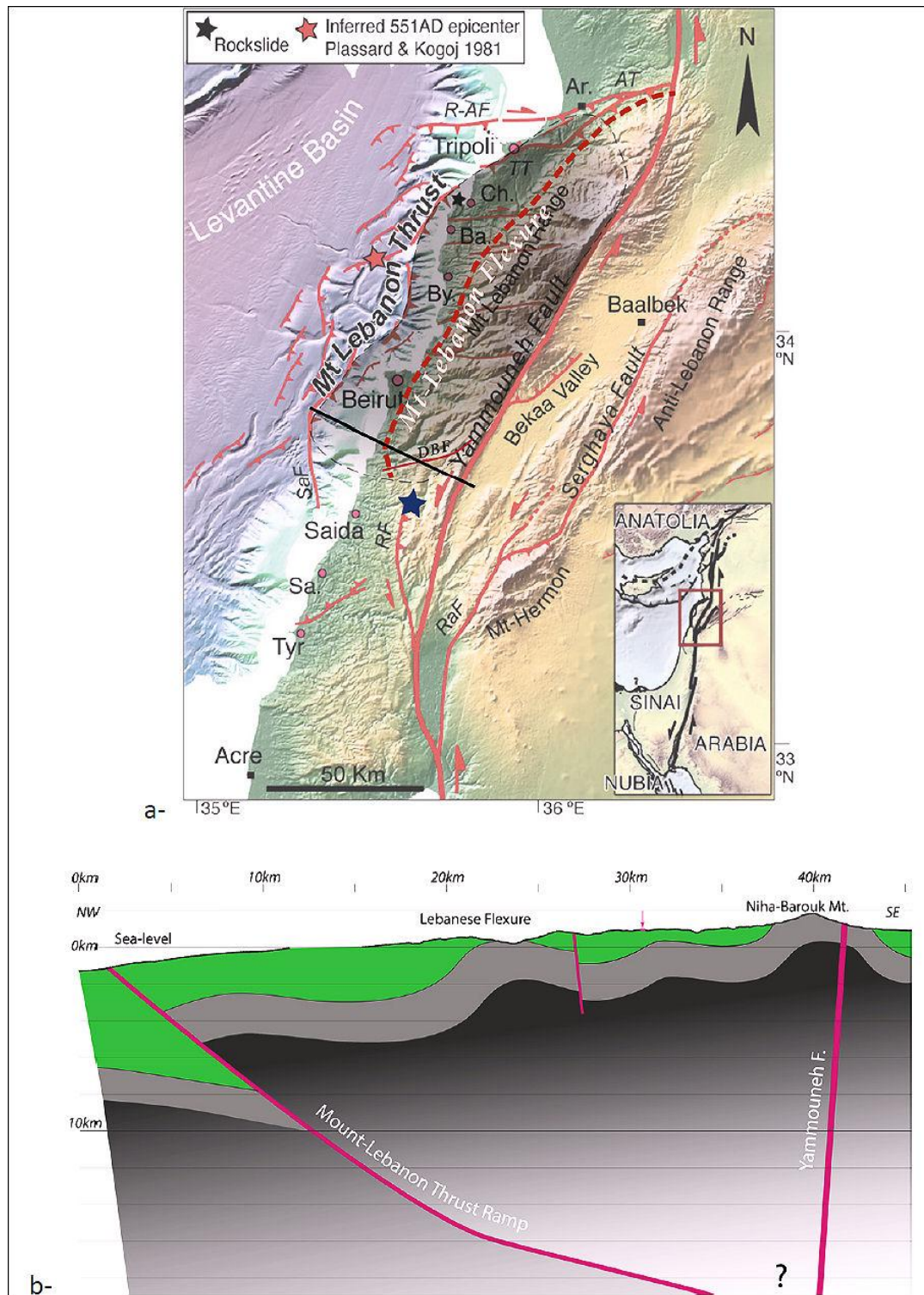


Figure 8. (a) Regional neo-tectonic map. Red lines are for active faults. Dashed red line is for the Mt-Lebanon Flexure. Gray shadow represents the ramp surface of the MLT in the sub-surface. Bisri Dam site (blue star) within the tectonic map of Lebanon. (RF= Roum Fault; DBF= Damour Beiteddine Fault), (b) Interpretative NW-SE cross-section of Mt-Lebanon showing the deep structure of the range (Elias, 2014).

4. SEISMICITY

The Dead Sea region has been affected by numerous moderate to large magnitude earthquakes over the course of history. Despite the lack of large earthquakes during the instrumental period, historical records suggest a substantial seismic activity (e.g. Ambraseys et al., 1994; Ambraseys and Jackson, 1998).

Three earthquakes stand out in the history of seismic activity in Lebanon: the earthquakes of 551 A.D., 1202 A.D and 1759 A.D. The magnitudes of these earthquakes were estimated based on historical accounts, to be in excess of 7.0, and caused devastating destruction in most coastal cities including Beirut, as well as the ancient city of Baalbeck inland (Sadek and Harajli, 2007). According to Ambraseys and Barazangi (1989), during the last millennium alone, more than 8 strong earthquakes with magnitude greater than 6.5 have struck along the northern continuation of the Dead Sea fault in Lebanon and Syria.

A schematic map of main active faults and the major historical earthquakes of Lebanese restraining bend is provided in Figure 9 after Daeron et al. (2005). Figure 10 (after Ferry et al., 2011) illustrates the seismicity of the historical and instrumental periods along the Dead Sea Transform fault, whereas Figure 11 presents the catalogue of the post-1900 period compiled for the EMME project (Zare et al., 2014), together with the location of the Bisri Dam.

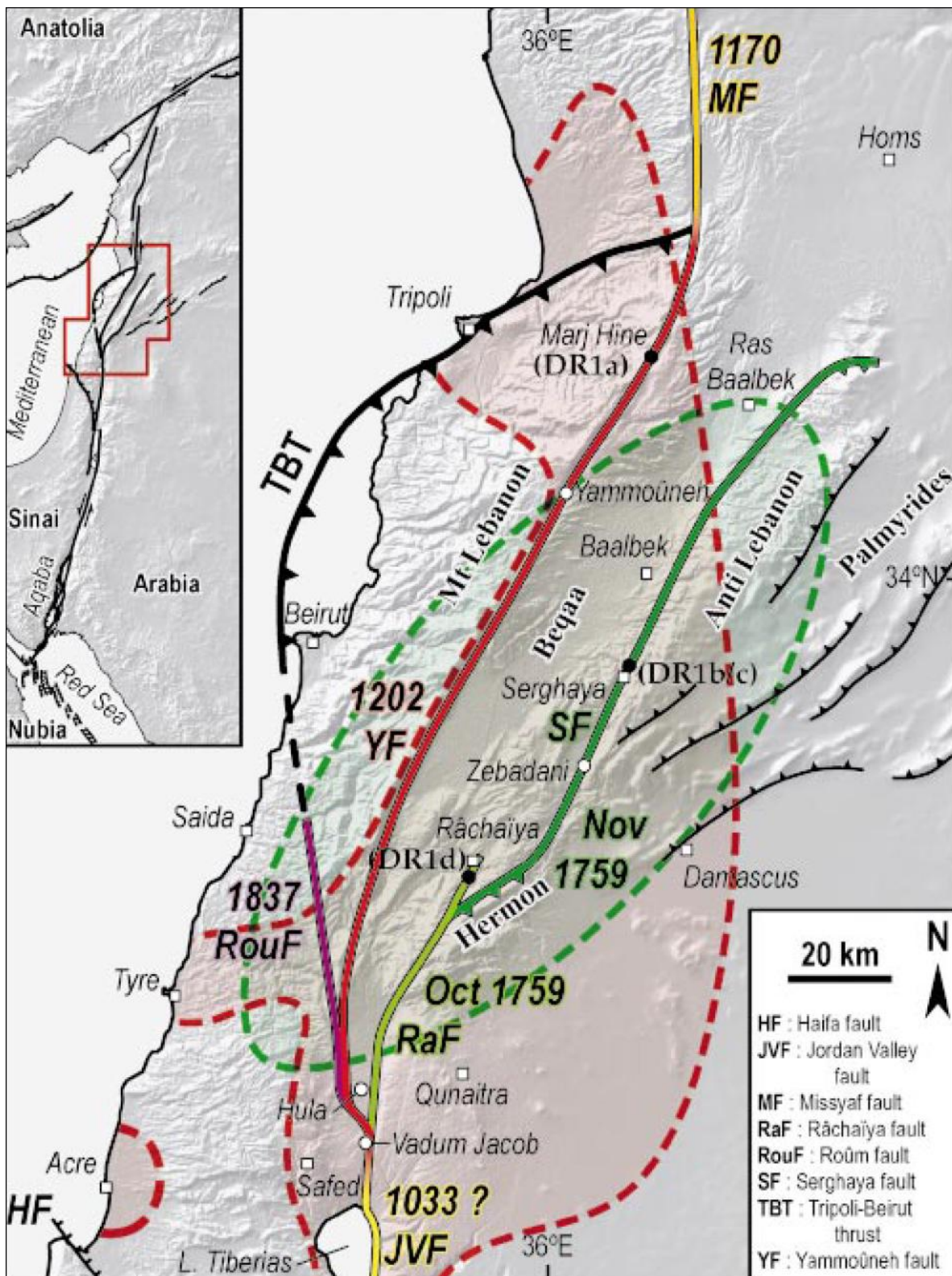


Figure 9. Main active faults and the major historical earthquakes. Bold colored lines show maximum rupture lengths of large historical earthquakes in past 1000 years. Bold dashed lines enclose areas where intensities VIII were reported in A.D. 1202 (red) and November 1759 (green) according to Ambraseys and Melville (1988) and Ambraseys and Barazangi (1989) (after Daeron et al., 2005).

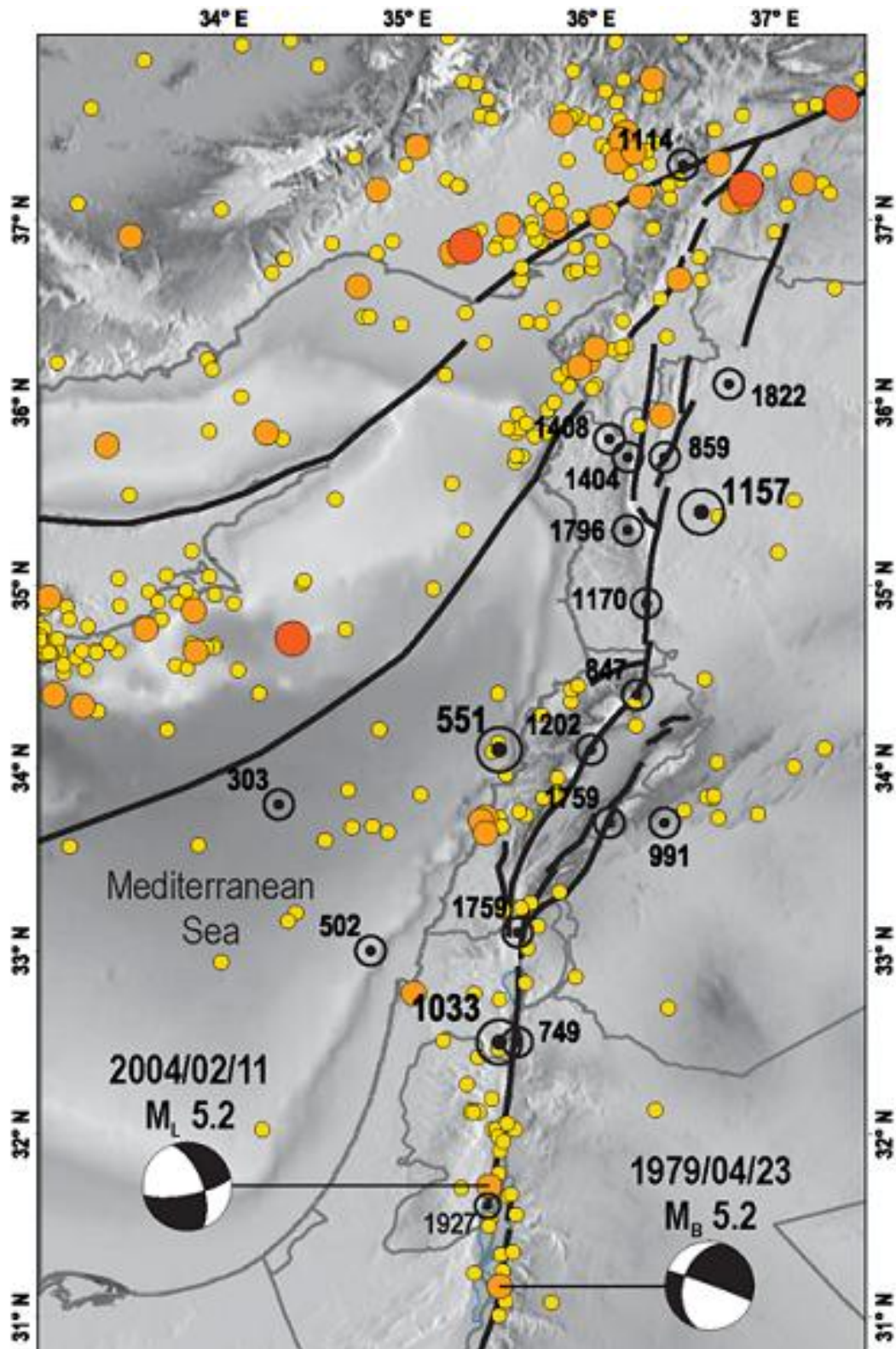


Figure 10. Seismicity of the Dead Sea Transform system (after Ferry et al., 2011). Instrumental events with $M \geq 4$ from 1964 to 2006 (IRIS Data Management Center); Historical events with $I \geq VII$ (Ambraseys and Jackson, 1998; Sbeinati et al., 2005) in open circles.

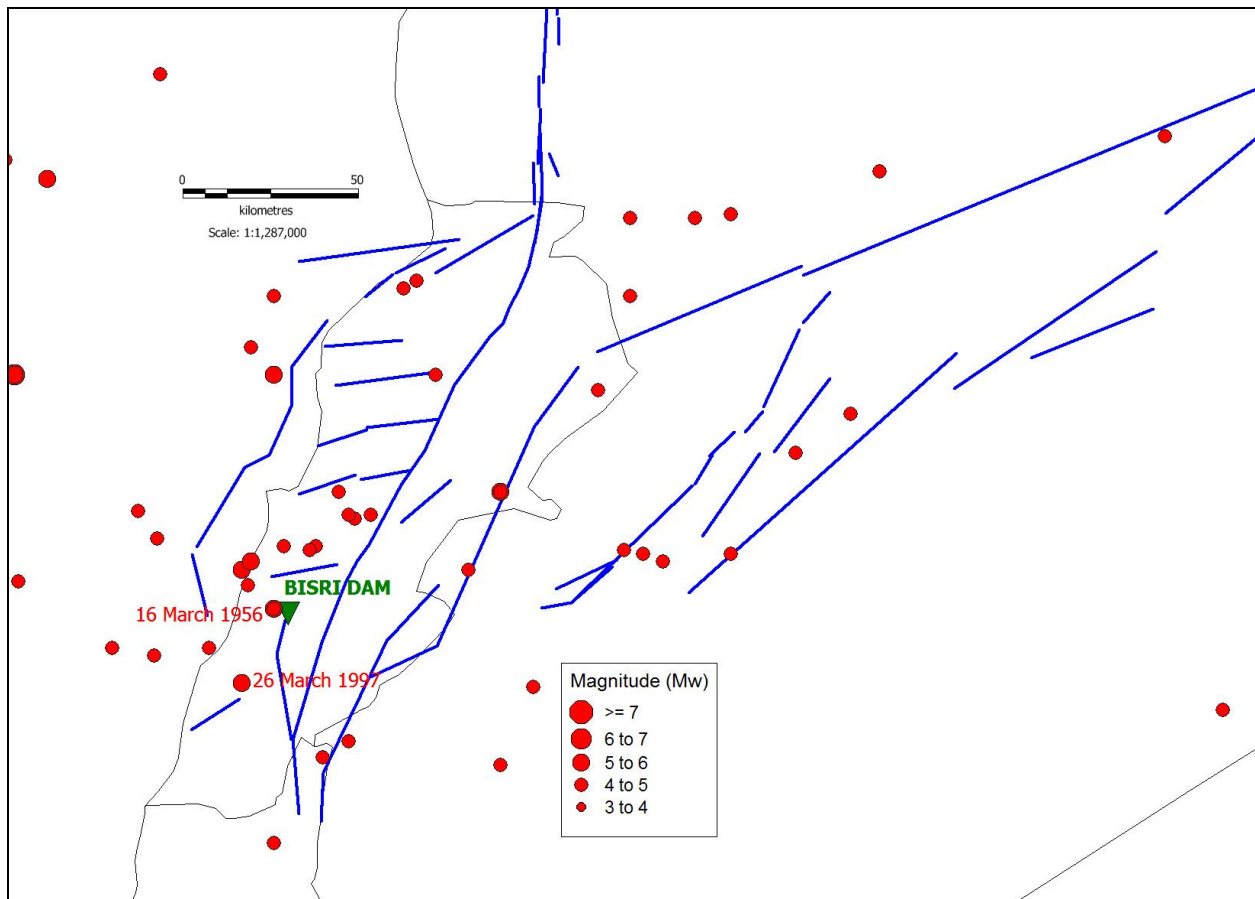


Figure 11. The earthquake catalogue of the region for the period 1900 – 2006 (Zare et al., 2014). Blue lines represent the active fault database compiled for the EMME project.

The Rour Fault which is a secondary branch of the Plate Boundary that splays into the Lebanon at Huleh south has exhibited considerable seismic activity (e.g. Girdler, 1990; Butler, 1997; Darawcheh et al., 2000; Khair, 2001).

The instrumental seismicity (ISC, NEIC, EMSC bulletins) shows a scatter of moderate earthquake epicentres around the Rour Fault with one relatively important event, namely the double shock of 16 March 1956 (Ms 4.8, 5.1). This earthquake left 136 dead, 6000 homes destroyed and about 17000 heavily damaged. More recently, an earthquake of magnitude 5.3 struck Lebanon on March 21, 1997 (Figure 11). The earthquake reached Beirut with an intensity of about VI on the Modified Mercalli (MM) intensity scale and resulted in high levels of shaking for a short duration of about 6 seconds (Sadek and Harajli, 2007)

A magnitude 6.4 or larger earthquake on January 1, 1837 was felt in towns near the site, and aftershocks were felt for at least three months following the main shock (Ambraseys, 1997). From the damage distribution (Figure 12) the source of these events associated with the Rour Fault. However, even though this event seems to have been large enough to produce surface ruptures, no field observations have yet indicated that such ruptures exist (Ambraseys, 1997).

This event as reviewed by Ambraseys (1997):

- caused damage in a narrow zone which extended from Saida to Marjayun, Bshara and Lake Tiberias,
- claimed 3,000 victims
- is associated with three large aftershocks (Jan. 16, 22 and May 20, 1837)
- is likely associated with rupture on the Rour fault and its S continuation W of the Hule

- no conclusive evidence of surface faulting
- has an estimated magnitude of 7.0.

The palaeoseismic study conducted by Nemer and Meghraoui (2006) shows the occurrence of at least 4-5 large seismic events with surface ruptures associated with the Roub Fault during the last 10510 years, the last event being post 84-239 AD (Nemer and Meghraoui, 2006). It is believed that the 1 January 1837 earthquake is the most likely candidate for being the most recent large seismic event along the Roub Fault. A slip-rate of 0.86-1.05 mm/year was derived. Nemer and Meghraoui (2006) further states that the potential of the Roub Fault for producing large earthquakes similar in magnitude to that of 1837 must be taken into consideration within any seismic hazard study of the region.

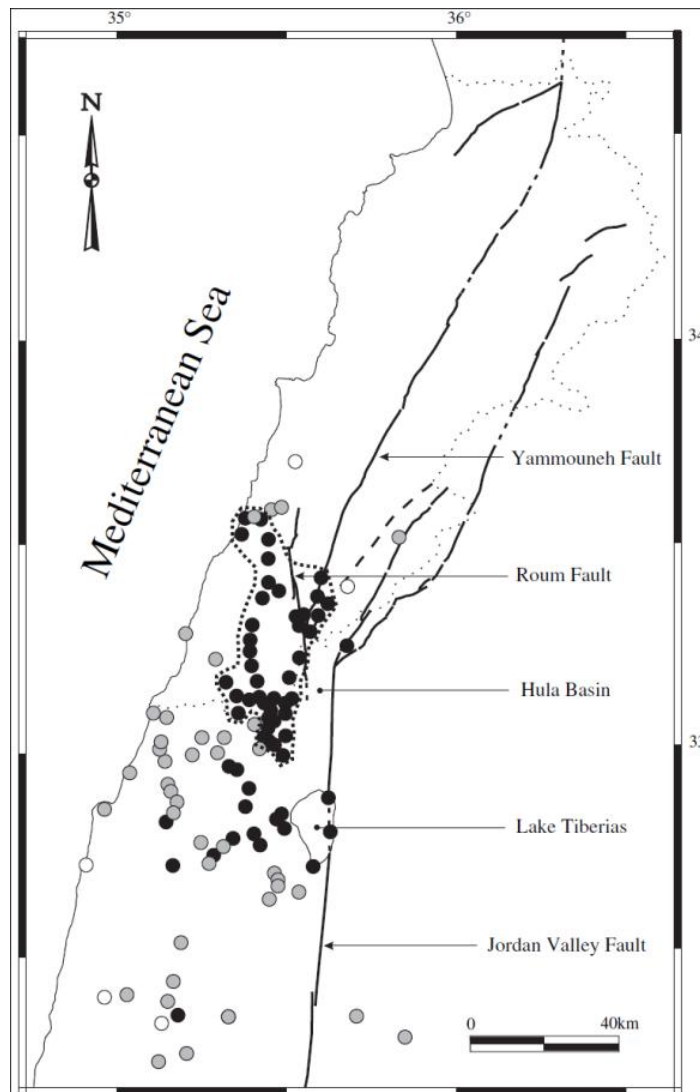


Figure 12. The epicentral region of the 1837 earthquake (after Nemer and Meghraoui, 2006; modified from Ambraseys, 1997). Circles indicate near-field locations of affected sites. Black, grey, and white circles correspond to MSK intensities of VIII, VII, and VI, respectively. Dotted contour bounds the area of concentrated maximum damage.

Although lacking seismic activity in the 20th century, recent paleoseismic investigations have indicated that the Yammouneh Fault, which is the main strand of the Dead sea Transform

Fault in Lebanon, is tectonically active and has ruptured in infrequent but large earthquakes ($M > 7.0$) (e.g., Daron et al., 2005, 2007; Nemer et al. 2008), including the Ms 7.6 event in 1202 (Figure 13). Another major event is the Ms 7.4 November 25, 1759 earthquake, which occurred on the Serghaya Fault, to the East of the Yammouneh Fault (Figure 14). Despite the apparent lack of present day seismicity, all recent studies reviewed suggested that the Yammouneh Fault is more likely to accommodate most of the plate motion within the Lebanese restraining bend (e.g., Gomez et al., 2003; Daron et al., 2004; Gomez et al., 2007).



Figure 13. Map of intensity distribution for May 20, 1202 earthquake (Ambraseys and Melville, 1988, figure from Sbeinati et al., 2005). Shaded zone is the most affected region.

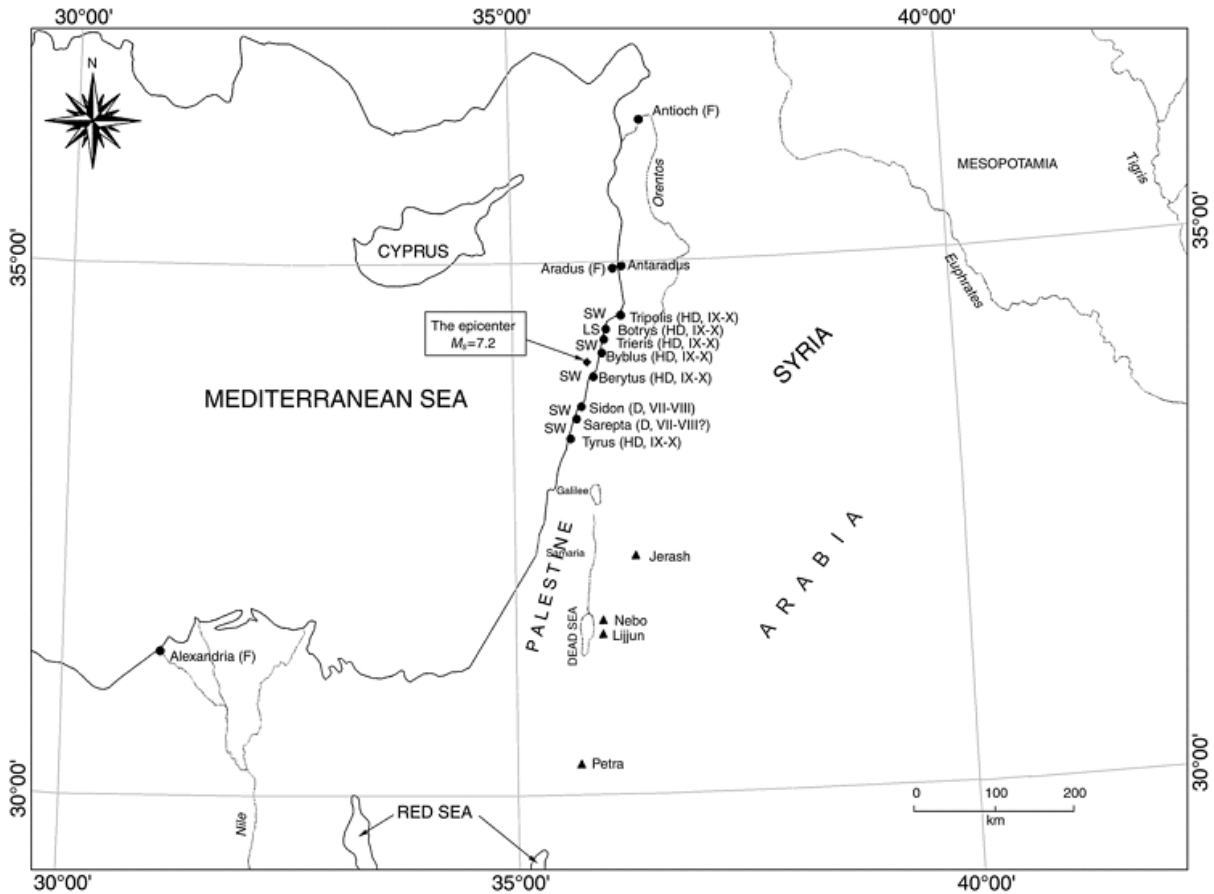


Figure 15. Map of intensity distribution for July 9, 551 A.D. earthquake. F – felt; D – damage; LS – landslide, and SW – Sea-Wave. Triangles represent possible damaged archaeological sites (Darawcheh et al., 2000; figure from Sbeinati et al., 2005).

5. GROUND MOTION PREDICTION EQUATIONS

Ground-motion prediction equations (GMPEs) relate a ground-motion parameter to a set of explanatory variables describing the earthquake source, wave propagation path and local site conditions. These independent variables include magnitude, source-to-site distance and some parameterization of local site conditions, and often style-of-faulting and hanging wall effects. The seismic hazard analysis is faced with the difficult task of deciding which GMPEs to use for a given project, since the resulting predicted spectra are strongly dependent on the GMPEs chosen.

In today's understanding the main separation of the GMPE's are based on the three major tectonic regimes: active crustal regions (ACRs); subduction zones (SZs); and stable continental regions, (SCRs) (Douglas, 2011 and Douglas et al., 2012). In this connection, Bommer et al. (2010) state that the first basis for exclusion of a GMPE model is that it is from a tectonic region that is not relevant to the location of the site for which the hazard assessment is being conducted.

The Next Generation Attenuation (NGA) project developed a series of GMPEs intended for application to geographically diverse regions (substantially from Taiwan, California, and Europe/Turkey); the only constraint is that the region be tectonically active with earthquakes occurring in the shallow crust. The NGA GMPEs are presented by Abrahamson and Silva

(2008), Boore and Atkinson (2008), Campbell and Bozorgnia (2008), Chiou and Youngs (2008), and Idriss (2008). An important issue for many practical applications is whether ground motions or GMPEs for one region can be applied to another. Rigorous comparative studies conducted by Campbell and Bozorgnia (2006), Stafford et al., (2008) and Scasserra, et al. (2009) and the GMPE studies of Akkar and Bommer (2010) indicate that the NGA-GMPEs are applicable and can be utilized for earthquake hazard in assessment Europe.

Due to the lack of recorded strong motion data in and around Lebanon, no comparisons could be made between the existing GMPEs and actual recordings near the site. The region where the Bisri Dam is located essentially qualifies for the ACR type tectonic regime. As such, we will first review the pre-selected GMPEs that would be appropriate to use for the earthquake hazard assessment for the Bisri Dam.

In connection with the Global Earthquake Model (GEM, www.globalquakemodel.org) the following three models were selected (Stewart et.al, 2014) for Active Crustal Regions: Akkar and Bommer (2010), Chiou and Youngs, (2008), and Zhao et al. (2006). These models provide a good geographical spread (respectively, one for Europe and the Middle East, one global, and one predominantly for Japan). Although, the Boore and Atkinson (2008) model was seriously considered for selection as an alternative or supplement to the Chiou and Youngs (2008), the Chiou and Youngs (2008) was preferred over the other pre-selected NGA models because its magnitude-scaling and its anelastic attenuation term were considered to be more appropriate than the other NGA models.

The GMPEs that are chosen in the context of a regional GEM project (SHARE; Seismic Hazard Harmonization in Europe, www.share-eu.org) for Shallow Crustal Active Regions were: Akkar and Bommer (2010) Cauzzi and Faccioli (2008) Zhao et al. (2006) Chiou and Youngs (2008) with the respective weights of 0.35, 0.35, 0.1 and 0.2, to be employed in the logic-tree analysis (Delavaud et.al, 2012a,b).

Under the framework of the Earthquake Model of the Middle East (EMME, www.emme-gem.org) project (a regional project of GEM, that provided a uniform assessment of the seismic hazard and risk in the Middle East and Caucasus region) the ground motion prediction equations (GMPEs) applicable in the region were studied (Erdik et al, 2012). The overall seismotectonic features of the EMME region suggest the consideration of shallow active crustal (SACR) and subduction regions (SR) for seismic hazard calculations. For establishing the GMPE logic-tree for SACRs in EMME, a total of 14 ground-motion predictive models, that fulfill the pre-selection criteria set by Cotton et al. (2006), were selected as candidate GMPEs and were subjected to two analytical testing and ranking methods using a subset of EMME strong-motion (SM) databank, almost exclusively consisting of ground-motions compiled from the SACRs in EMME territory (Kale and Akkar, 2012). The overall performances of Akkar et al. (2014), Chiou and Youngs (2008), Akkar and Cagnan (2010) and Zhao et al. (2006) were found relatively better than the rest of the candidate GMPEs. For the GMPE logic-tree in EMME hazard assessments these GMPEs were used with weights of 0.35, 0.35 0.20 and 0.1 respectively.

On the basis of this review it would be appropriate to use the GMPEs of Akkar and Bommer (2010), Chiou and Youngs (2008) and Boore and Atkinson (2008) for the deterministic assessment of the earthquake hazard at the Bisri dam site. In addition to being identified by GEM, SHARE and EMME projects Akkar and Bommer (2010) and Akkar et al. (2014) are the only GMPEs that are essentially based on the Middle East data. Among these two ground motion prediction models, we suggest Akkar and Bommer (2010) to be more appropriate to be used for the DSHA study of Bisri Dam, as this model also includes the magnitude dependent standard deviation term. As such it will be given a weight of 0.5 in the logic tree

combination of DSHA results from the selected GMPEs. On the other hand both Chiou and Youngs (2008) and Boore and Atkinson (2008) are based on an international database that includes more data of large magnitude near fault strike slip earthquakes, similar the deterministic earthquake scenarios considered for the Bisri Dam. In the logic tree combination both of the NGA GMPEs Chiou and Youngs (2008) and Boore and Atkinson (2008) will be assigned a relative weight of 0.25.

6. PROBABILISTIC SEISMIC HAZARD ANALYSIS

6.1. PREVIOUS STUDIES

Previous studies on the seismic hazard of the region surrounding Bisri Dam by different agencies and independent researchers provide a comparison with the results of this study. Commonly, available reports and maps focus on peak ground acceleration (PGA) at return periods of 475 years and 2,475 years. Unless noted, the site conditions utilized by these previous reports are unknown.

The Global Seismic Hazard Assessment Program (GSHAP) estimates peak ground acceleration (PGA) value at Bisri Dam of approximately 0.2g-0.3g for a 475-year return period (Grünthal et al., 1999).

A study of earthquake hazard of Jordan and the surrounding areas by Jimenez et al. (2008) indicates that Bisri Dam is located in a zone associated with PGA values of 0.2g to 0.25g for a 475-year return period.

Al-Tarazi and Sandoval (2007) estimate a PGA value of 0.2g for a 475-year return period in the Bisri Dam site for firm rock.

Seismic hazard maps produced for the U.S. Agency for International Development Assessment for Building Codes Project (Shapira and Hofstetter, 2007) show the site located in an area corresponding to PGA values of 0.2g to 0.25g for a 475-year return period at generic bedrock.

A study of seismic hazard for Lebanon by Hujier et al. (2011) shows a PGA value of approximately 0.25g for a 475-year return period and 0.35g for a return period of 950 years at the Bisri Dam site.

Another study of seismic hazard for Lebanon by Elnashai and El Khoury (2004) shows a PGA value of 0.18g for a 475-year return period and 0.25g for a return period of 2,500 years.

6.2. THE PSHA MODEL USED IN THIS STUDY

EMME (Earthquake Model of Middle East) Project (www.emme-gem.org) is a comprehensive undertaking that aimed to develop a homogenous hazard model for the Middle East Region combining both local, regional and international expertise. American University of Beirut (AUB) was the local partner of the project in Lebanon, together with Rafiq El-Khoury and Partners. The active fault database, the earthquake catalogue and the fault and areal source models of the region have been compiled and developed with the contribution of Dr. Ata Elias from AUB.

The source zonation model of EMME has two distinct branches, one being the areal source (AS) model and the second being the fault source + background seismicity (FS) model.

Poissonian, (i.e. earthquake occurrence without memory) approach has been adopted in the hazard modelling. The AS model assumes that the seismicity is homogeneously distributed over each delineated source zone and the magnitude –frequency distribution for each source zone is obtained based on the Gutenberg-Richter earthquake recurrence model, using the homogenized and declustered catalogue of the region (Zare et al., 2014). The FS model has two components: the fault sources and the background seismicity. The active fault database of the region compiled within the project has been used to develop a fault source model, in which segments of the active fault database are converted to linear sources, each defined by top and bottom depths, dip and rake angles, Mmax and slip rates. Earthquakes with magnitude 6 and higher are assumed to occur on fault sources and the activity rate for the fault sources is determined from the slip rate. To complete the fault source model in the regions where faulting information is not available (either by lack of faults or by lack of information) the background seismicity is used. The earthquake catalogue of the post-1900 period is used to obtain smoothed seismicity model with a grid spacing of 0.1 degrees and a smoothing distance of 25 km using the method proposed by Frankel et al. (1996). Within the buffer zones of the fault sources only earthquake rates for magnitude less than 6 are obtained from the smoothed seismicity as the higher magnitude contributions are assumed to come from the fault sources. For regions outside the buffer zones of the fault sources, all activity is obtained from smoothed seismicity.

As defined in Section 5 of this report, the GMPE logic tree for the PSHA study is defined as Akkar et al. (2014), Chiou and Youngs (2008), Akkar and Cagnan (2010) and Zhao et al. (2006) were found relatively better than the rest of the candidate GMPEs. For the GMPE logic-tree in EMME hazard assessments these GMPEs were used with weights of 0.35, 0.35, 0.20 and 0.1 respectively.

Figure 16 presents the AS and FS models of the EMME project for the Bisri Dam region. The 0.1 degree grid sources representing the background seismicity of the FS model are not shown on the figure.

To compute the hazard at the Bisri Dam site, the AS and FS models have been assigned, as in the EMME project, weights of 0.6 and 0.4 respectively. The final results are obtained using the logic tree structure composed of the source model and GMPE levels. Figure 17 presents the hazard curves obtained for PGA, and spectral accelerations for T=0.2 sec and T=1.0 sec at the Bisri Dam site from the EMME model. The values obtained for return periods of 72, 144, 475 and 2475 years are also summarized in Table 1. The uniform hazard spectrum corresponding to 144 years return period is provided in Figure 18.

Table 1. PSHA results for the Bisri Dam site

Return Period (years)	AS (%60) + FS (%40)		
	PGA (g)	SA (T=0.2 sec) (g)	SA (T=1.0 sec) (g)
72	0.142	0.315	0.072
144	0.213	0.483	0.113
475	0.419	0.983	0.251
2475	0.781	1.890	0.528

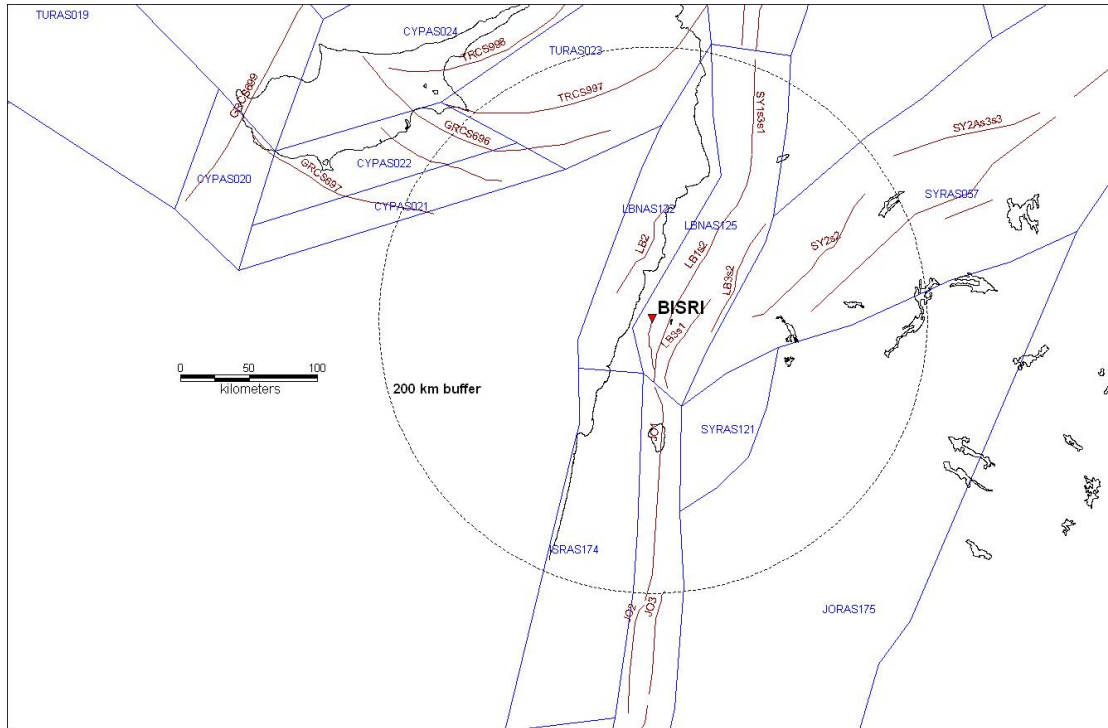


Figure 16. EMME Source zonation model. Both areal and fault source models are shown on the figure.

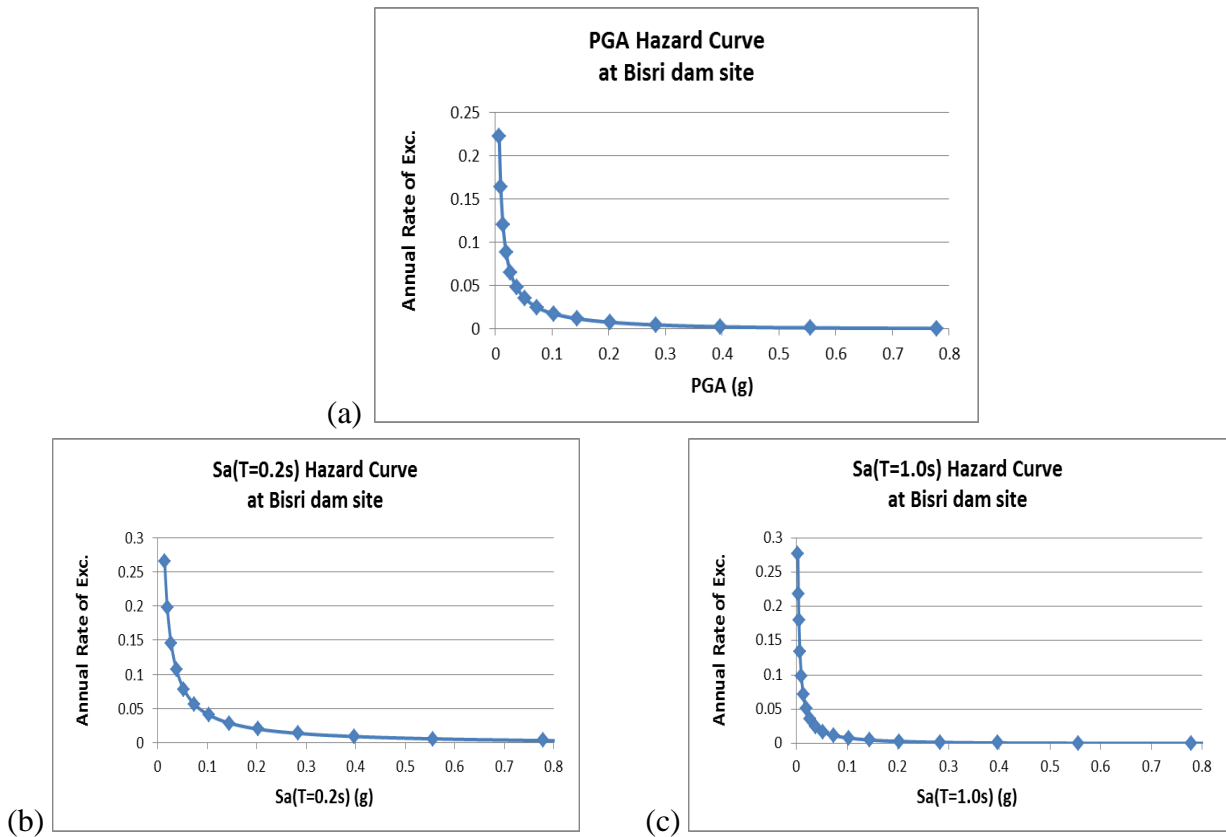


Figure 17. Hazard curves for the Bisri Dam site. (a) PGA, (b) SA (T=0.2 sec) and (c) SA (T=1.0 sec).

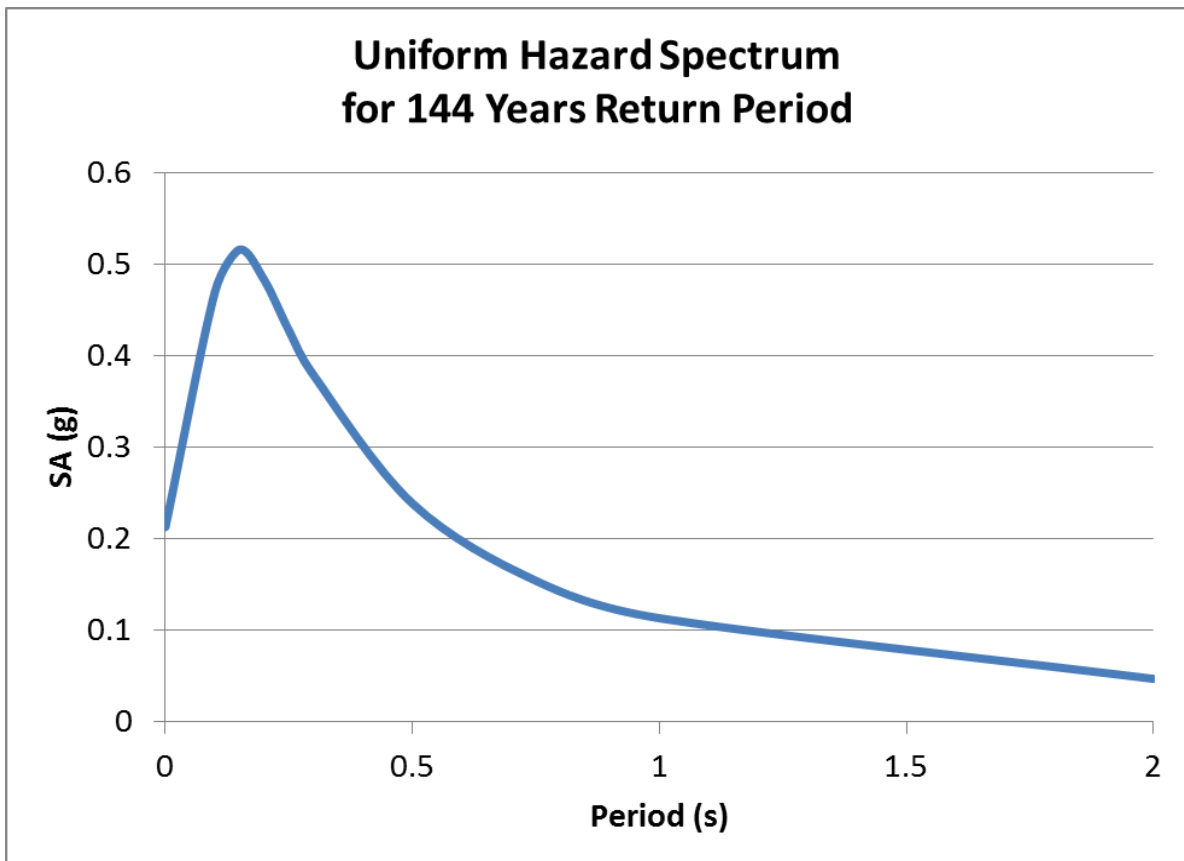


Figure 18. Uniform Hazard Spectrum corresponding to 144 years return period for the Bisri Dam site.

Differences between previous ground motion estimates and values from this PSHA likely result from a combination of the use of different ground motion prediction models, and how crustal faults are dealt with by each study. We note that a majority of the available previous studies do not account for the potential contribution of discrete fault sources to the seismic hazard, but use only historical seismicity to define the regional hazard. We also note that the available previous studies were completed prior to the recent investigations of slip rate for the Yammounh fault (eg., Gomez et al., 2007; Daëron et al., 2004) and therefore do not incorporate the slip rates and maximum magnitude estimates that are greater than previously available.

7. VERTICAL RESPONSE SPECTRA FOR 144 YEAR RETURN PERIOD

Today the preferred approach for obtaining the response spectrum of the vertical component of motion is to scale the horizontal spectrum by vertical-to-horizontal (V/H) spectral ratios. Bommer et.al (2011) has developed a model for the prediction of V/H ratios for peak ground acceleration and spectral accelerations from 0.02 to 3.0 s is developed from the database of strong-motion accelerograms from Europe and the Middle East (**Error! Reference source not found.**). The predicted ratios are found to be in broad agreement with recent models derived from predominantly western North America data (such as, Gülerce and Abrahamson, 2011).

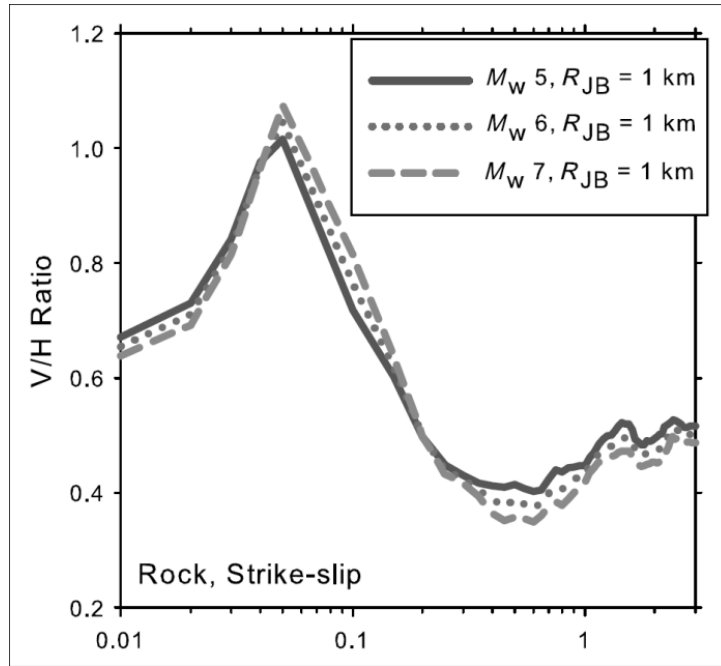


Figure 19. Median V/H spectra for different magnitude ranges and distance = 1km (after Bommer et.al, 2011).

The vertical response spectra corresponding to 144 years return period for the Bisri Dam site was developed by applying the appropriate vertical/horizontal (V/H) ratios, from the Bommer et.al (2011) relationships, to the horizontal design basis spectra is presented in Figure 20.

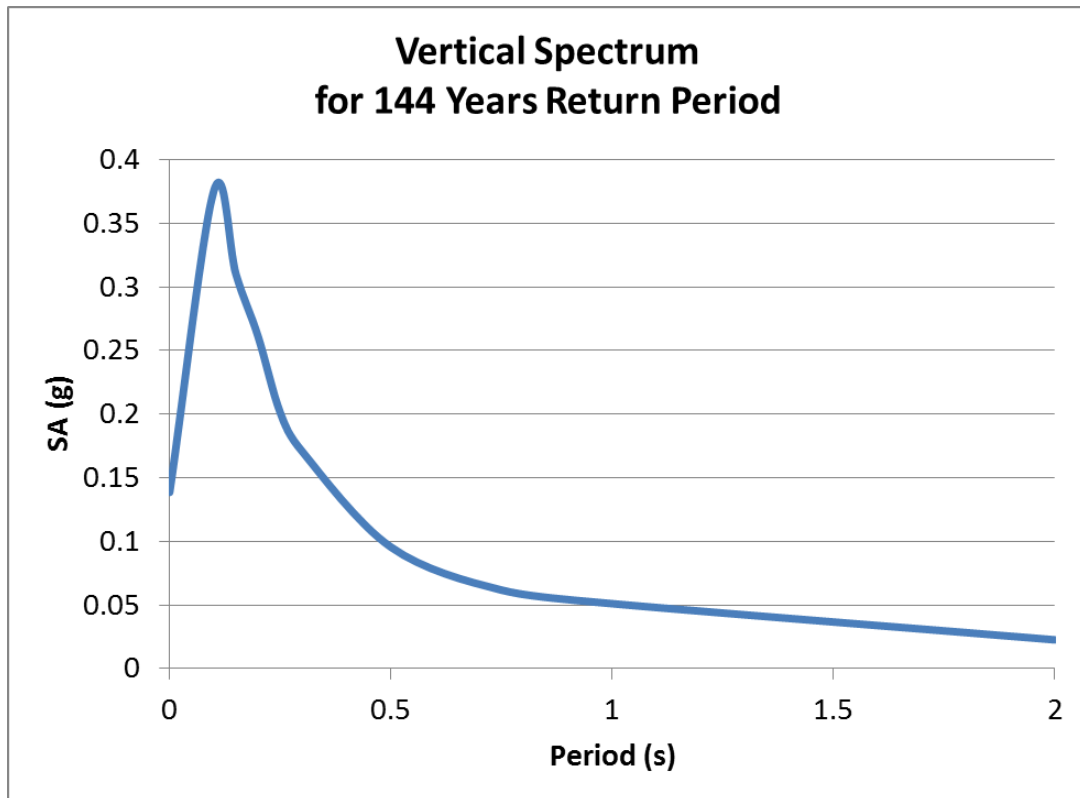


Figure 20. Vertical response spectrum corresponding to 144 years return period, obtained using coefficients after Bommer et.al, 2011).

8. DETERMINISTIC SEISMIC HAZARD

M_{MAX} defines the upper limit of the earthquake recurrence relationship for the source as well as the magnitude levels that would be used in the deterministic earthquake hazard assessment (DSHA). The appropriate and careful selecting of the M_{MAX} is much more important in the DSHA since together with the site-to-source distance it is the most important parameter that would control the earthquake hazard at the site. An evaluation of M_{MAX} for all fault sources was made using empirical relationships that relate fault rupture length and rupture area to maximum magnitude (Wells and Coppersmith, 1994; Ellsworth, 1999, 2003; Hanks and Bakun 2002,2008; Shaw (2008) and; Strasser et.al (2010). Wells and Coppersmith (1994) provide the following formula for strike slip faults, with a standard deviation of 0.28 magnitude units:

$$\text{Mean } M_{max} = 5.16 + 1.12 \log L \quad (1)$$

Where L (in km) is the length of the fault rupture. In practice the mean value of the M_{max} is used and L is taken as a certain percentage (generally, 50% to 75%) of the total fault length. A plot of M_{MAX} versus the fault rupture area (A , in km^2) based on the results of widely considered researches are provided in Figure 21 for strike slip faults.

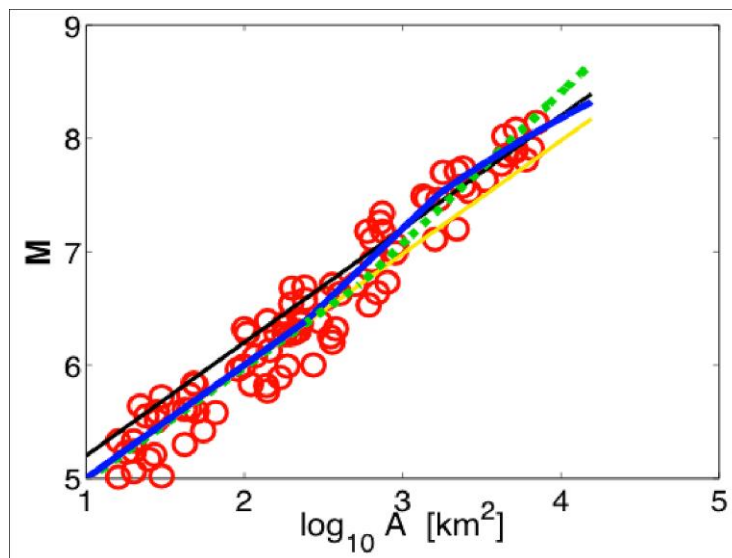


Figure 21. M (magnitude)– $\log A$ (area) Data and Relations: Wells and Coppersmith (1994). (Yellow) Ellsworth (1999, 2003) (black). Hanks and Bakun (2002,2008) (Green). Shaw (2008) (Blue). (After Shaw, 2008).

The maximum magnitude earthquake associated with the Roum fault, at a distance of only 2km from the Bisri Dam, will certainly control the earthquake hazard at the dam site. It appears that the previous assessments of the M_{max} on the Roum Fault simply (and very conservatively) were obtained as 7.3 by adding 0.3 units to the historical maximum magnitude (M_7 , 1837 earthquake). It should be noted that the M_7 is only an estimate and 0.3 is an ad-hoc value.

For the Roum Fault, even assuming the whole length of the fault will rupture at the maximum magnitude earthquake (this is a very conservative assumption), Equation 1 provides a mean M_{max} of $M_w 6.9$. Taking $L=35$ km and the Fault Width as $W=20$ km the Fault Rupture Area A on the Roum Fault can be computed as 700 km². As the average of expressions provided in Figure 21 the mean of the maximum magnitude can be computed as $M_w=7$,

which is essentially identical to the estimated magnitude of the 1837 earthquake. The deterministic earthquakes considered in this analysis are:

- Mw7.9 strike-slip earthquake on the Yammouneh Fault at 12km from the site.
- Mw7.8 thrust (reverse) earthquake on the MLT Ramp at 35km from the site.
- Mw7 strike-slip earthquake on the Roum Fault at 2km from the site.

As it can be seen with the exception of MMAX on the Roum Fault, which was re-assessed as Mw7, all the three scenarios are as same as that provided by Elias (2014).

Results of the deterministic analysis results for these three scenarios are presented in Figure 22 for the 84-percentile (i.e. median+1 standard deviation) response spectra on NEHRP-B type soil ($V_{s30}=760\text{m/s}$) using the GMPE model of Akkar and Bommer (2010). As it can be clearly assessed the Roum Fault scenario governs the earthquake hazard at the Bisri Dam site.

The deterministic median+1SD response spectra obtained for the Roum Fault scenario using selected AB2010 (Akkar and Bommer, 2010), CY2008 (Chiou and Youngs, 2008) and BA2008 (Boore and Atkinson, 2008) GMPE's for NEHRP B type site class are provided in Figure 23. The average median+1SD response spectra, obtained using logic tree combination of these results with relative weights of 0.50, 0.25 and 0.25 respectively for the GMPEs of AB2010, CY2008 and BA2008 is provided in Figure 24.

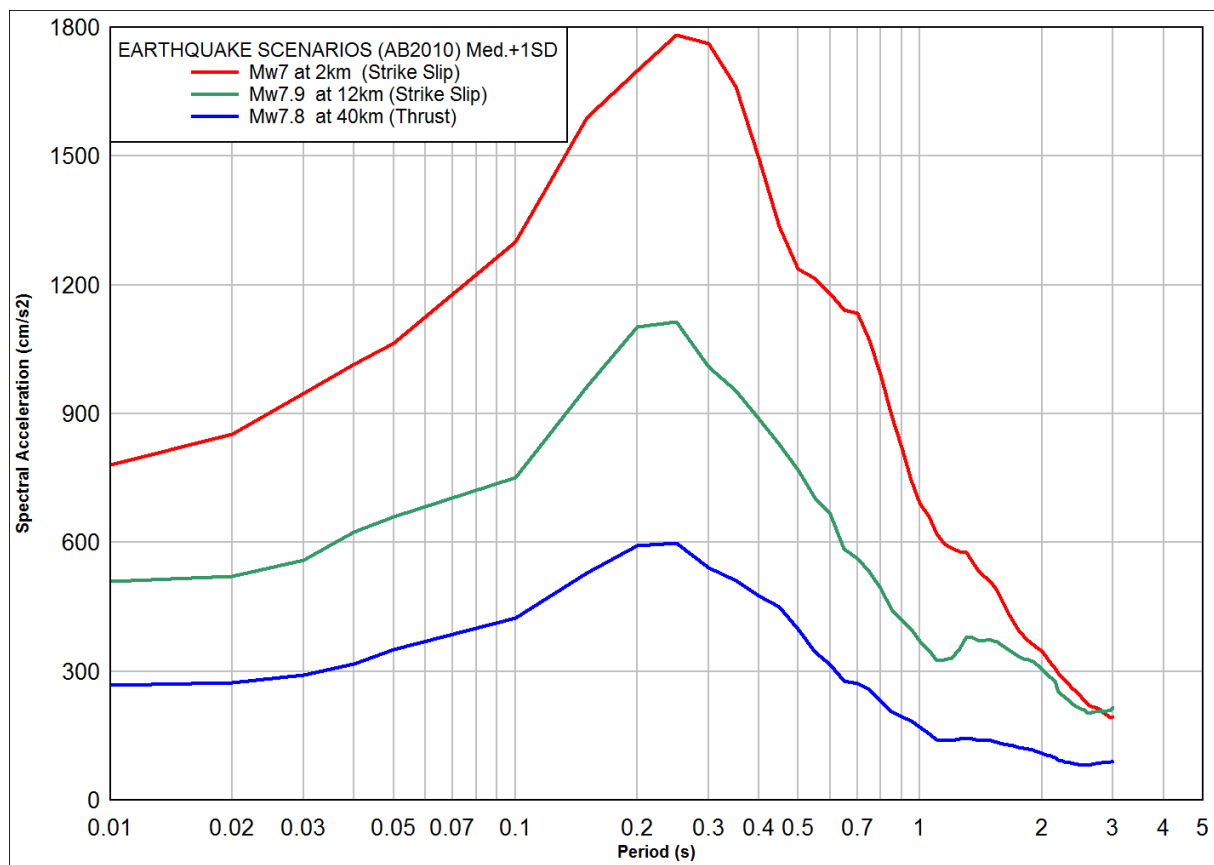


Figure 22. Deterministic Median+1SD (84-percentile) response spectra using AB2010 GMPE for NEHRP B type site class. Red: Mw7 strike-slip earthquake on the Roum Fault at a distance of 2km from the site; Green Mw7.9 strike-slip earthquake on the Yammouneh Fault at a distance of 12km from the site; Blue Mw7.8 thrust (reverse) earthquake on the MLT Ramp at a distance of 40km from the site.

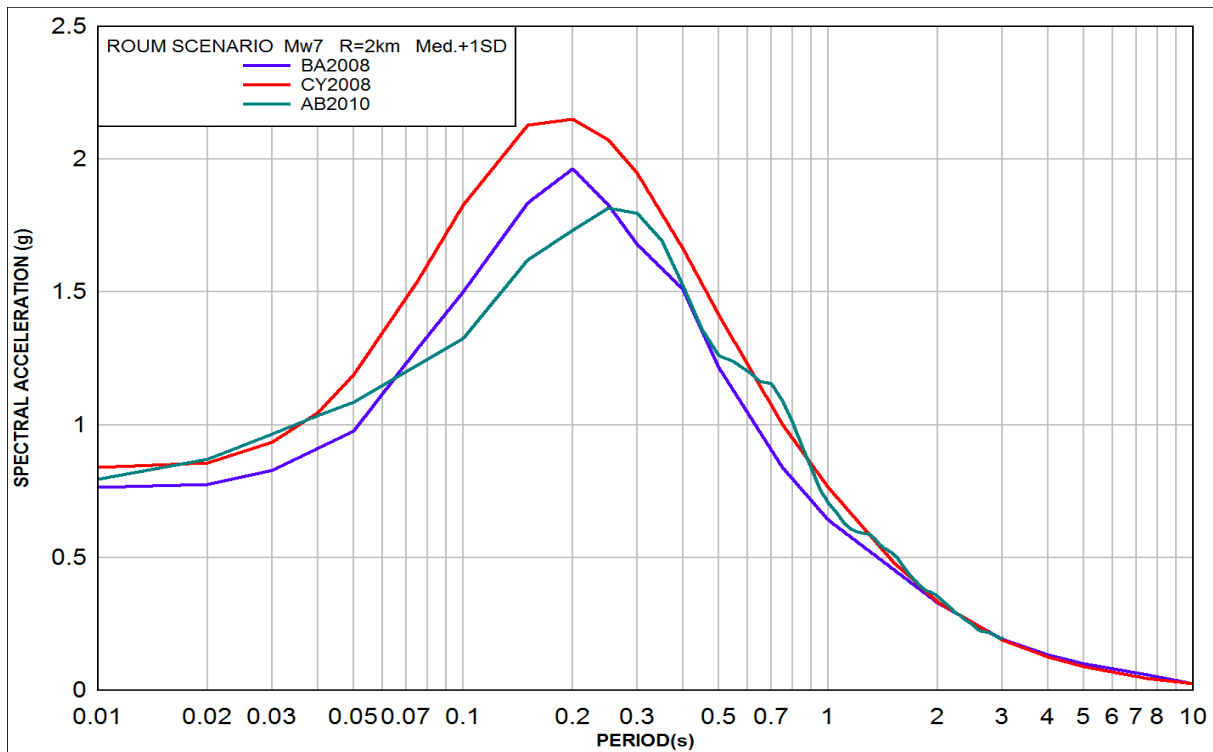


Figure 23. Median+1SD response spectra for Mw7 strike-slip earthquake on the Roum Fault at a distance of 2km from the site (NEHRP B site class) associated with BA2010, CY2008 and BA 2008 GMPE.

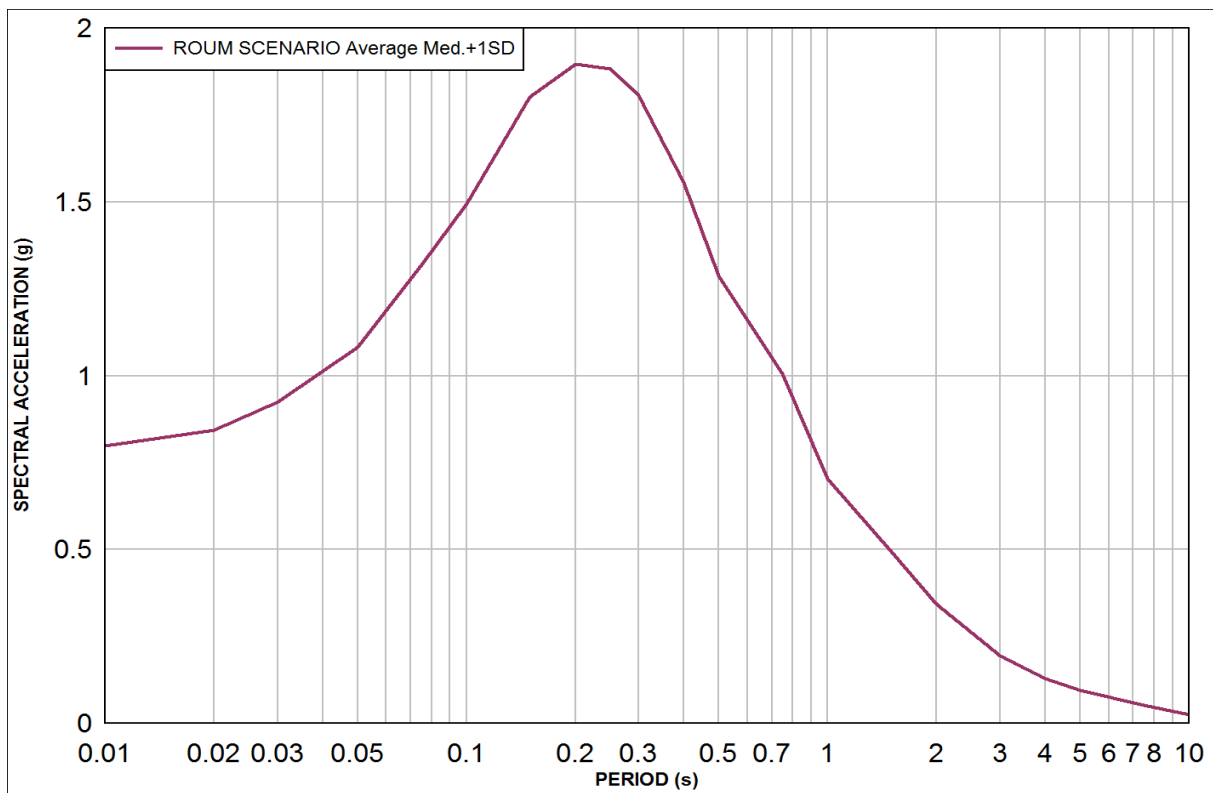


Figure 24. The average median+1SD response spectra for the Mw7 strike-slip earthquake on the Roum Fault at a distance of 2km (NEHRP B site class).

9. DIRECTIONALITY EFFECTS

Common methods to quantify spectral acceleration two-component horizontal shaking are to take the geometric mean of the spectral accelerations of the two as-recorded ground motion components (SaGM), to take the maximum spectral acceleration observed when looking over all horizontal orientations (SaRotD100), or to take the median spectral acceleration observed when looking over all horizontal orientations (SaGMRotI50).

Most of the recent GMPEs use either SaGM or SaGMRotI50, which are approximately equal to each other. The Shahi and Baker (2012) study have shown that SaGMRotI50 predictions should be multiplied by approximately 1.2 at short periods ($T < 0.1s$) and approximately 1.3 at longer periods ($T > 1s$) to yield SaRotD100.

Among the current earthquake resistant design codes, including the ICOLD design criteria, the specifics of whether to use SaGMRotI50 or for the design basis response spectra is not provided with the exception of ASCE 7-10 (2010), where SaRotD100 is specified.

Noting that the earthquake resistant design process for dam bodies already incorporates adequate levels of conservatism, the use of either SaGM or SaGMRotI50 will be considered for the assessment of the design basis response spectra of the Bisri Dam.

10. NEAR FAULT EFFECTS

The GMPEs used in the analysis do not explicitly differentiate near-fault effects; thus, it is necessary to modify the results to account for near-field fault rupture effects. These effects (termed Directivity Effects and Polarization) are important at periods of vibration longer than 0.5s are associated with large magnitude ($\geq MW 6.5$) earthquakes occurring on nearby faults, which essentially represent the case with the Roum Fault scenario.

Ground Motion Directivity

During an earthquake event, fault rupture propagation and earthquake source radiation pattern cause spatial variation of horizontal ground motions in amplitude and duration around the fault. Forward directivity occurs when rupture propagates toward the site, and the slip direction of the fault is aligned with the site (Somerville et al. 1997). In this situation, seismic energy radiated from the fault arrives at the site in a short time interval, resulting in a large pulse of motion at the beginning of the record. The velocity pulse is oriented in the fault-strike-normal direction due to polarization. Directivity effects increase spectral accelerations at locations where the rupture has propagated towards the site of interest "forward-directivity", for periods longer than approximately 0.5 seconds (Baker et. al, 2012). As the current GMPEs do not explicitly include directivity effects several directivity models have been developed to account for the near source ground motion characteristics (Somerville et al., 1997; Abrahamson, 2000; Rowshandel, 2006; Spudich et al., 2004; Spudich and Chiou, 2008; Rowshandel, 2010; Shahi and Baker, 2011).

Somerville et al. (1997) provide a simple empirical model (which was later modified by Abrahamson, 2000) to predict ground motion amplification, duration and polarization due to directivity effects. Spudich and Chiou (2008) developed a physically-based directivity model using isochrone theory, with an improved characterization of directivity that can be used to include the directivity modification to the NGA GMPEs. The average horizontal spectral acceleration from an empirical attenuation relation without directivity effect (Sa) can be modified to obtain the spectral acceleration with directivity effects (Sadir) by the following equation:

$$\ln Sa_{dir} = \ln Sa + f_D, \quad \text{or} \quad Sa_{dir}/Sa = \exp(f_D) \quad (2)$$

where the factor f_D is used to quantify the directivity effects. The directivity modification factors that predict directivity-induced variations of spectral acceleration provided by Spudich and Chiou (2008) for strike-slip faults are similar to those of Abrahamson (2000) and are roughly half of the factors predicted by Somerville et al. (1997).

Assuming full forward directivity (the Mw7 earthquake starts at the far end of the Roum Fault and ruptures the whole 35km length of the fault towards the Bisri Dam, located at 2km away from the end of fault) the Sa_{dir}/Sa values (modification factors) are computed using the Spudich and Chiou (2008) model as shown in Table 2. The factors are taken as the average values associated with AB2006 and CY2006 GMPEs.

Table 2. Directivity modification factors for the SEE level design basis response spectrum

Periyod (s)	0.5	0.75	1.0	1.5	2.0	3.0	4.0	5.0	7.5	10.0
Sa_{dir}/Sa	1.00	1.07	1.13	1.20	1.27	1.38	1.49	1.57	1.73	2.12

The response spectra modified for the directivity effects is provided in Figure 25.

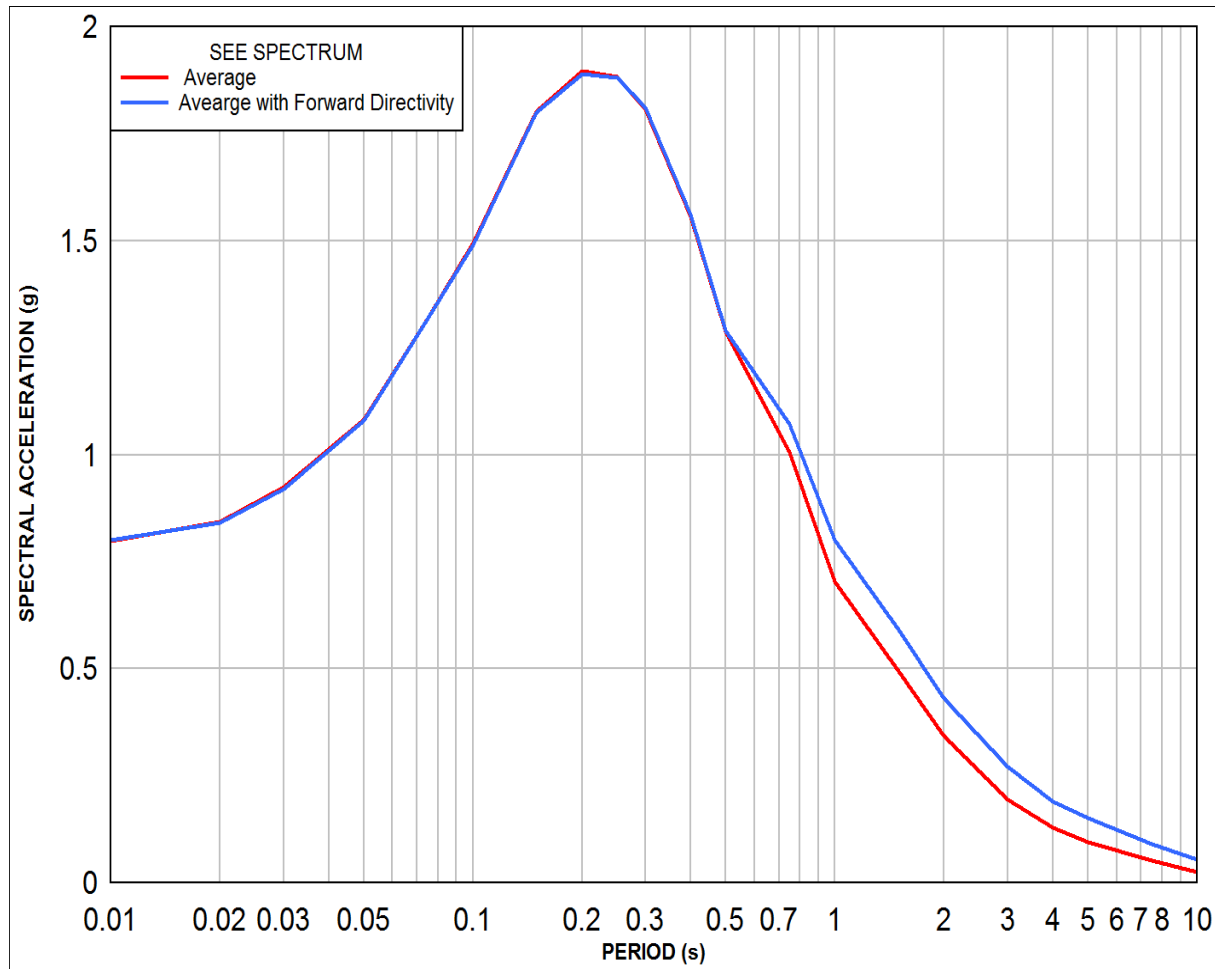


Figure 25. The average (Red, actually Figure 24) and the directivity modified design basis response spectra (Blue). Note that the directivity modification applies only first periods greater than 0.5s.

There also exist systematic differences (called “polarization”) of horizontal motions in the directions perpendicular (normal) to the fault strike (termed fault-strike-normal or fault-normal (FN) direction) and in the direction parallel to the fault strike (termed fault-strike-parallel or fault-parallel (FP) direction). The polarization of ground motion in the fault-strike-normal (FN) direction and the fault-strike-parallel (FP) direction caused by directivity effects depends primarily on earthquake magnitude and rupture distance. The ratio of fault-strike-normal to average horizontal motions is period-dependent, and may become significant at a period greater than 0.6 second, indicating a transition from incoherent source radiation and wave propagation conditions at short periods to coherent source radiation and wave propagation conditions at long periods (Somerville et al., 1997). For near-fault structures with very strong direction dependence in response the separation of FN and FP components is foreseen in ASCE 7-10 (2010). The effect of polarization of the ground motion is not considered in other current earthquake resistant design codes and in the ICOLD earthquake resistant design criteria.

11. DESIGN BASIS RESPONSE SPECTRA

On the basis of these evaluations and considerations the following design basis ground motion spectra can be provided:

The Operating Basis Earthquake is determined as the probabilistically assessed earthquake ground motion for an average return period of 144 years. The horizontal and vertical design basis spectra for the operating basis earthquake (OBE) for the random horizontal and vertical component are provided respectively in Figures 18 and 20. The response spectra is provided for 5% damping and for the free-field engineering bedrock outcrop.

The Safety Evaluation Earthquake is the maximum level of ground motion for which the dam should be designed or analyzed. For the earthquake resistant design of the Bisri Dam the SEE level ground motion will be determined to correspond to the 84-percentile deterministic MCE (i.e. median plus one standard deviation). The horizontal and vertical design basis spectra for the safety evaluation earthquake (SEE) for the random horizontal and vertical component are provided respectively in Figures 25 and 30. The response spectra is provided for 5% damping and for the free-field engineering bedrock outcrop.

12. SPECTRUM COMPATIBLE HORIZONTAL GROUND MOTION

When acceleration time histories (also referred to as accelerograms) of ground motions are required for the dynamic analysis of a structure, they should be developed to be consistent with the design response spectrum, as well as have appropriate strong motion duration for the particular design earthquake. In addition, whenever possible, the acceleration time histories should be representative of the design or safety evaluation earthquake in all the following aspects: earthquake magnitude, distance from source-to-site, fault rupture mechanisms (fault type, focal depth), transmission path properties, and regional and geological conditions. Since it is not always possible to find empirical records that satisfy all of the above criteria, it is often necessary to modify existing records or develop synthetic records that meet most of these requirements (NIST, 2011). Therefore, ground motion time histories are selected and scaled to enable response-history analysis that supports either design or performance assessment. The goals of analysis must be clearly understood must have a clear understanding of before choosing procedures to select and scale ground motions.

Since traditionally the seismic hazard at a site for design purposes has been represented by design spectra, virtually all modern seismic design codes and guidelines require scaling of selected ground motion time histories so that they match or exceed the controlling design spectrum within a period range of interest. As performance-based considerations become prerequisite in the seismic design and evaluation of building structures, the use of nonlinear response history analysis has gained importance. For this method, suites of appropriately selected and scaled (modified) ground motion records compatible with the target spectra are needed.

There are two general approaches to developing acceleration time histories: selecting a suite of recorded motions and synthetically developing or modifying one or more motions. The disadvantage is that the synthetic ground motions are not “real” motions. Real motions generally do not exhibit smooth spectra. Although a good fit to a design spectrum can be attained with a single accelerogram, it may be desirable to fit the spectrum using more than one accelerogram. Such motions have the character of recorded motions since the modeling procedures are intended to simulate the earthquake rupture and wave propagation process. For selecting recorded motions, it is necessary to select a suite of time histories (typically 3 or more) such that, in aggregate, valleys of individual spectra that fall below the design response spectrum are compensated by peaks of other spectra and the exceedance of the design response spectrum by individual spectral peaks is not excessive (preferably at least within the bandwidth of interest for structure specific analysis). For nonlinear analyses, it is desirable to have additional time histories because of the importance of (NIST, 2011).

The recently developed NGA GMPE relationships output an average horizontal spectral demand and the dispersion in that demand, where this average is the rotated geometric mean denoted as GMRotI50 (Boore et al., 2006). GM denotes the geometric mean of two horizontal components, Rot denotes that rotations over all non-redundant angles are considered, I denotes that period-independent rotations are used, and 50 identifies the prediction of median values. The geometric mean of two horizontal components of ground motions is calculated as the square root of the product of the two horizontal response spectral accelerations at each period of interest. The current USGS probabilistic ground motion maps (<http://earthquake.usgs.gov/hazards/designmaps/>) are based on the GMRotI50=geometric mean representation of horizontal ground motion

On the basis of these developments, ASCE 7-10 (2010) has changed how site specific ground motions will be developed. The relevant stipulations include:

- Where three-dimensional analyses are performed, ground motions shall consist of pairs of appropriate horizontal ground motion acceleration components that shall be selected and scaled from individual recorded events. Appropriate ground motions shall be selected from events having magnitudes, fault distance, and source mechanisms that are consistent with those that control the maximum considered earthquake.
- For each pair of horizontal ground motion components, a square root of the sum of the squares (SRSS) spectrum shall be constructed by taking the SRSS of the 5 percent-damped response spectra for the scaled components (where an identical scale factor is applied to both components of a pair).
- Each pair of motions shall be scaled such that in the period range from 0.2T to 1.5T, the average of the SRSS spectra from all horizontal component pairs does not fall below the corresponding ordinate of the response spectrum used in the design

- If seven or more pairs of ground motions are used for the response-history analysis, the average value of the response parameter of interest is permitted to be used for design.

Methods for the scaling of ground motion records vary from scaling the ground motion to a single period on the target spectrum, to average matching over a period range to operations involving frequency modification (Abrahamson, 1998) of the ground motion records to match the target spectrum. Since the frequency characteristics and the correlation between the components of the records remain unchanged the use of scaling procedures has gained increasing acceptance especially for long period structures exposed to near field and fault directivity effects.

Work by the PEER Ground Motion Selection and Modification Working Group (GMSM Working Group, 2009) has comprehensively studied the importance of the ground motion selection and spectrum compatible ground motion generation methodologies. The software tool developed by GMSM has opted for the scaling of the selected ground motion to fit to the target spectrum (Baker, 2011). This allows selecting recordings for which the geometric mean of the two horizontal components provides a good match to the target spectrum. The basic criterion is that the spectrum of the time series provides a “good match” to the user’s target spectrum over the spectral period range of interest. The quantitative measure used to evaluate how well a time series conforms to the target spectrum is the mean squared error (MSE) of the difference between the spectral accelerations of the record and the target spectrum. This approach produces scaled recordings that provide the best match to the spectral shape of the target spectrum over the user-specified period range of interest, but whose spectra will oscillate about the target. Minimization of the MSE is achieved by a scale factor given by the mean weighted residual in natural logarithm space between the target and the record spectra. Since MSE is computed over both components with the same value of/applied to both components, the relative amplitude of the two horizontal components as well as the vertical component is maintained.

Earthquake records in this database are sorted out on the basis of their geo-tectonic characteristics and combined with other worldwide data with similar geo-tectonic characteristics. Any earthquake (regardless of the political boundary in which it is located) is eligible, as long as the earthquake is related to the so called “shallow active crustal regions” regions of the world, and conform with the fault mechanisms, magnitude range and source distance range particular to the project. Within the database, ground motion records have been identified as having strong velocity pulses that may be associated with fault rupture directivity effects.

The seven sets of bi-axial earthquake ground motion records selected for scaling to the SEE level target spectrum are provided in Table 3. The selected records are listed according to the best fit in Table 3. The geometric mean of these two horizontal spectra of these 7 sets of scaled ground motion is plotted with the target spectrum in Figure 26 for SEE level target spectrum.

Table 3. Records selected for scaling to the SEE level target spectrum

Event	Year	Station	Magnitude	Mechanism	Rjb (km)	Rrup (km)	Vs30 (m/s)	Scale factor	Mean Square Error
Kocaeli, Turkey	1999	Gebze	7.51	strike slip	8	11	792	4.255	0.032
Chi-Chi, Taiwan-04	1999	CHY074	6.20	strike slip	6	6	553	1.978	0.044
Kocaeli, Turkey	1999	Izmit	7.51	strike slip	4	7	811	3.552	0.058
Morgan Hill	1984	Coyote Lake Dam -	6.19	strike slip	0	1	561	1.142	0.103
Morgan Hill	1984	Gilroy Array #6	6.19	strike slip	10	10	663	3.162	0.134
Duzce, Turkey	1999	IRIGM 487	7.14	strike slip	3	3	690	2.870	0.151
Darfield, New Zealand	2010	LPCC	7.00	strike slip	25	26	650	3.731	0.163

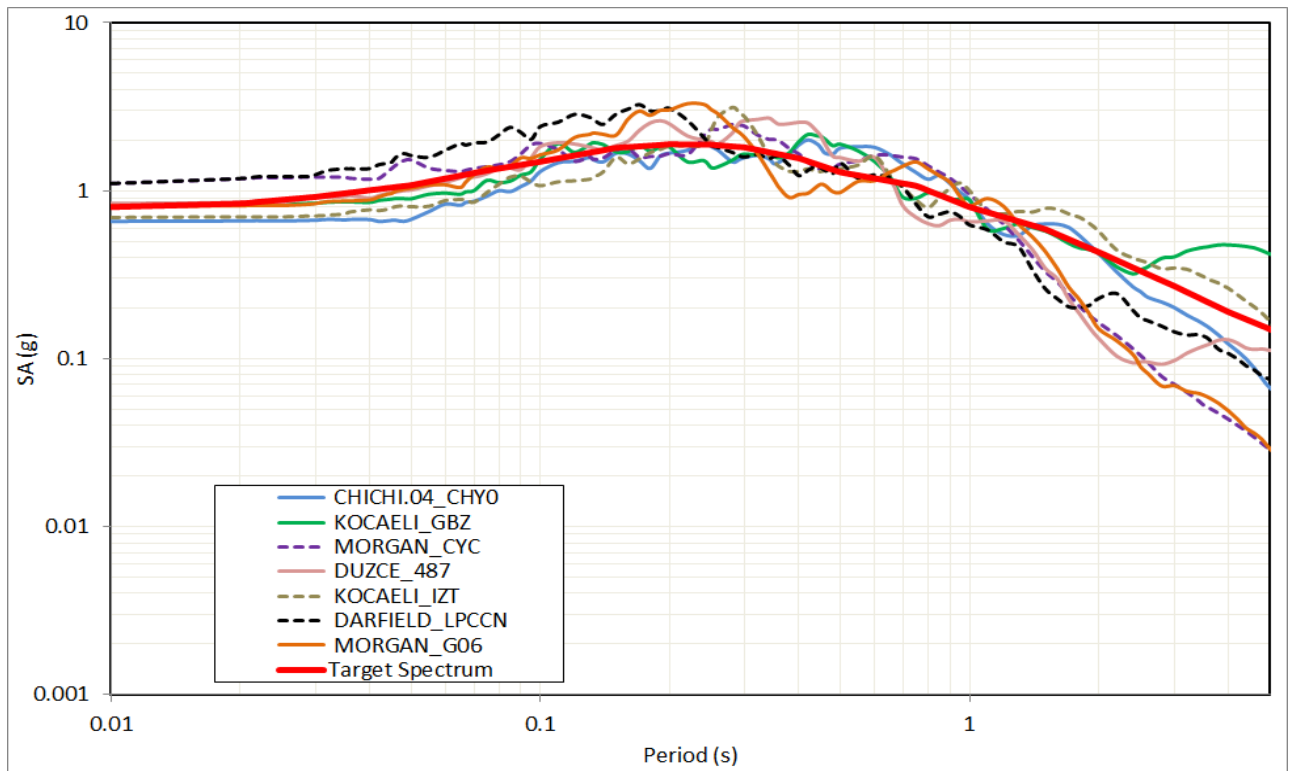


Figure 26. Geometric mean of horizontal spectra of the 7 sets (Table 3) of scaled ground motion and the SEE level target spectrum (Dashed lines correspond to first three best fit of scaled records at 0.5 s).

The geometric mean of two horizontal spectra of first three scaled ground motion records, that best fits to 0.5s at target spectrum, are plotted with this SEE level target spectrum in Figure 27.

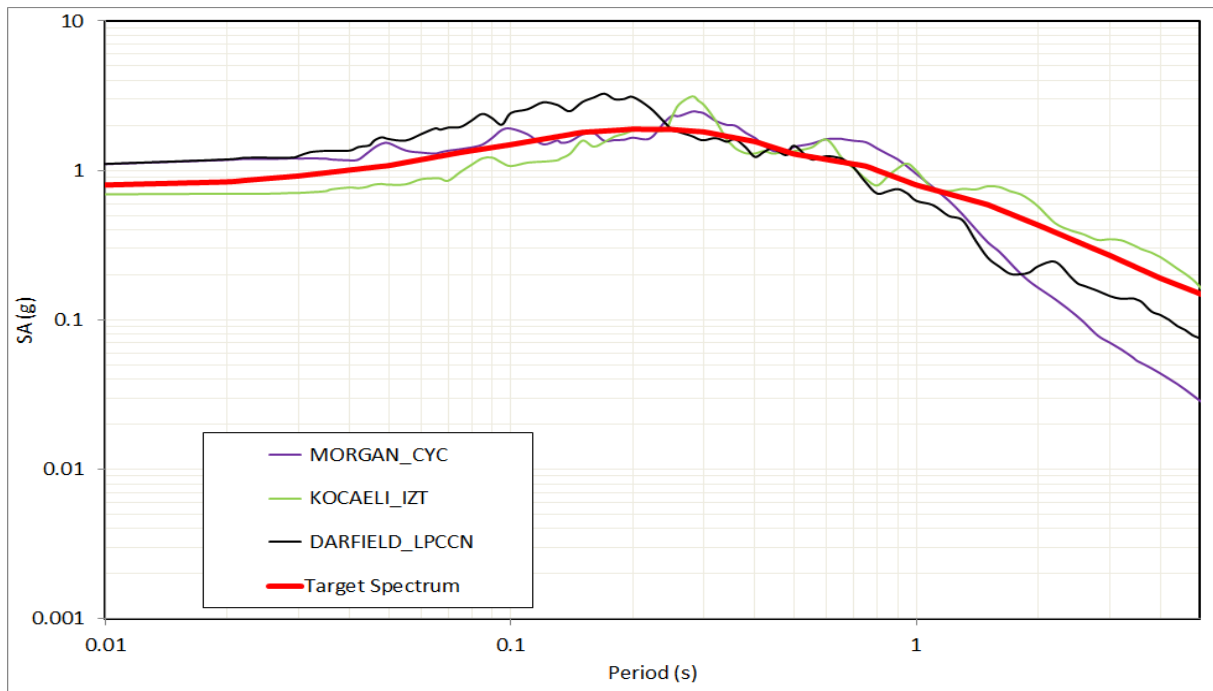


Figure 27. Geometric mean of horizontal spectra of first three best fit of scaled ground motion records at 0.5 s and the SEE level target spectrum.

The comparison of the geometric and arithmetic mean of the scaled spectra plotted on Figure 28 with the SEE level target spectrum is provided.

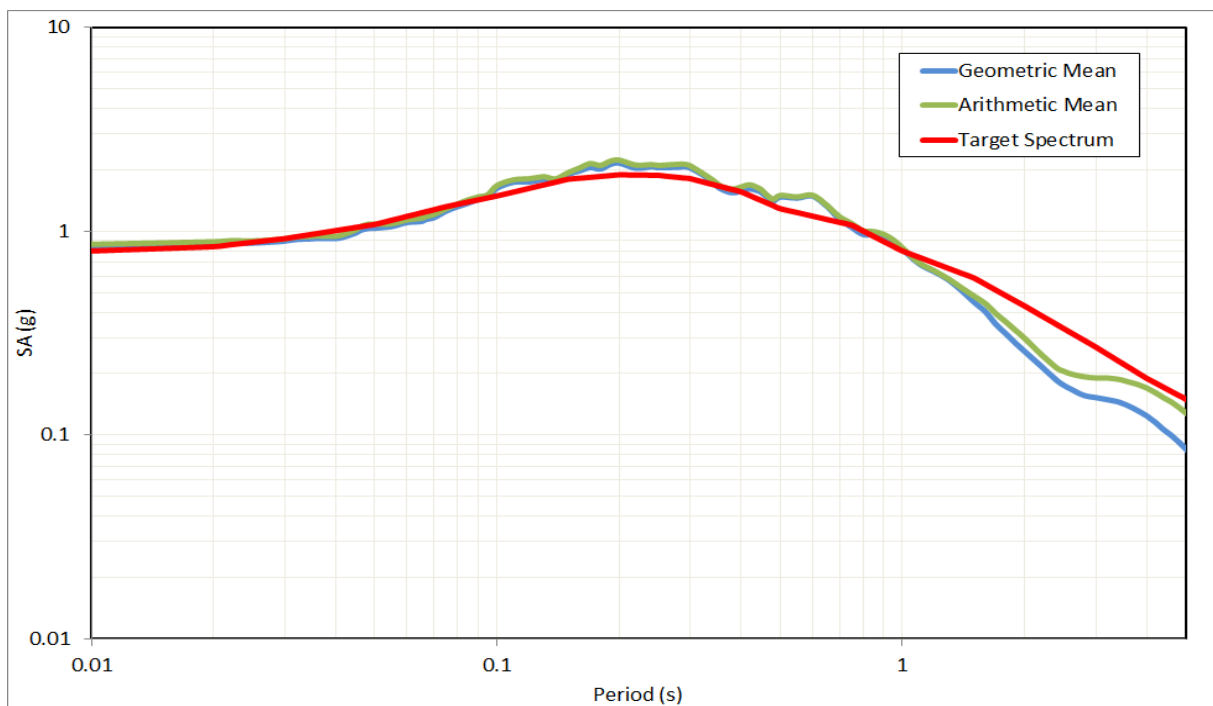


Figure 28. Comparison of the SEE level target spectrum with the geometric and arithmetic mean of the seven scaled horizontal spectra.

Seven vertical ground motion records of the selected earthquakes are scaled by the factors listed in Table 3. Average vertical spectrum of these seven vertical ground motion is shown in Figure 29.

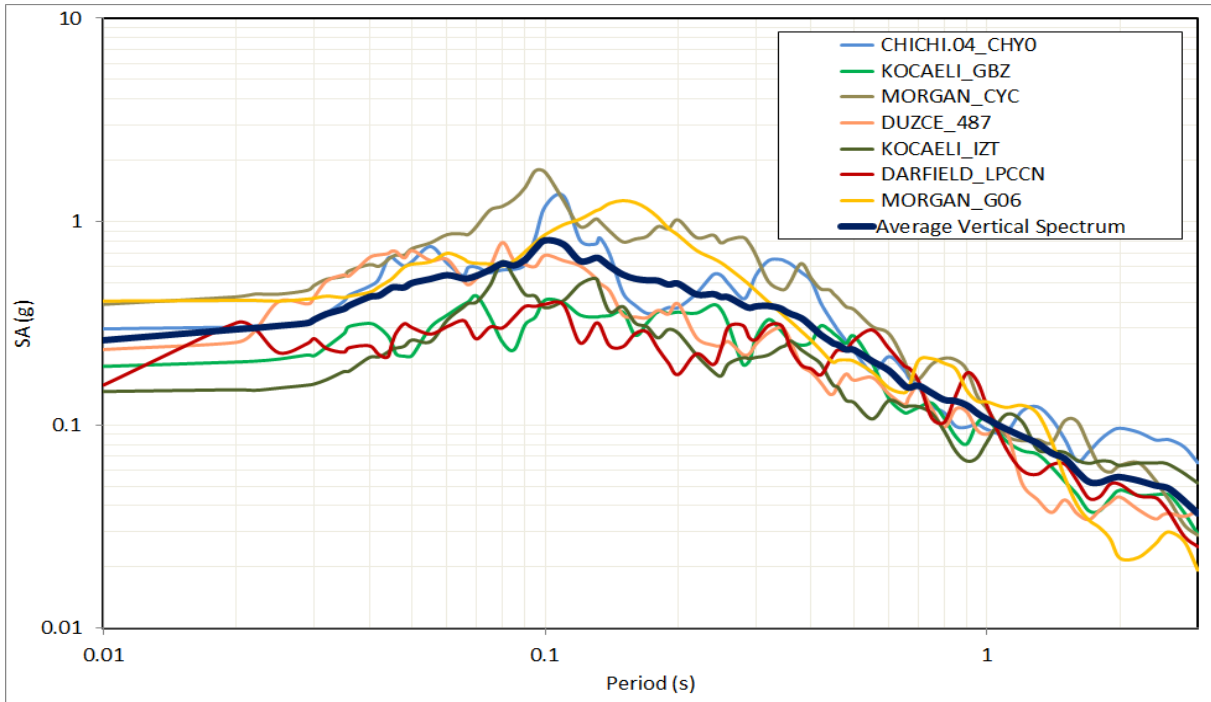


Figure 29. Average vertical spectrum of the 7 scaled vertical ground motion records.

The SEE level vertical response spectra for the Bisri Dam site can also be developed by applying the appropriate vertical/horizontal (V/H) ratios, from the Bommer et.al (2011) relationships, to the SEE level horizontal design basis spectrum, as illustrated in Figure 30. However, this spectrum will not necessarily be in conformity with the vertical components of the 7 sets of horizontal spectrum compatible scaled ground motion. Since the time domain analysis will be used for the SEE level design the vertical spectrum should preferably be taken as the average spectrum indicated in Figure 29.

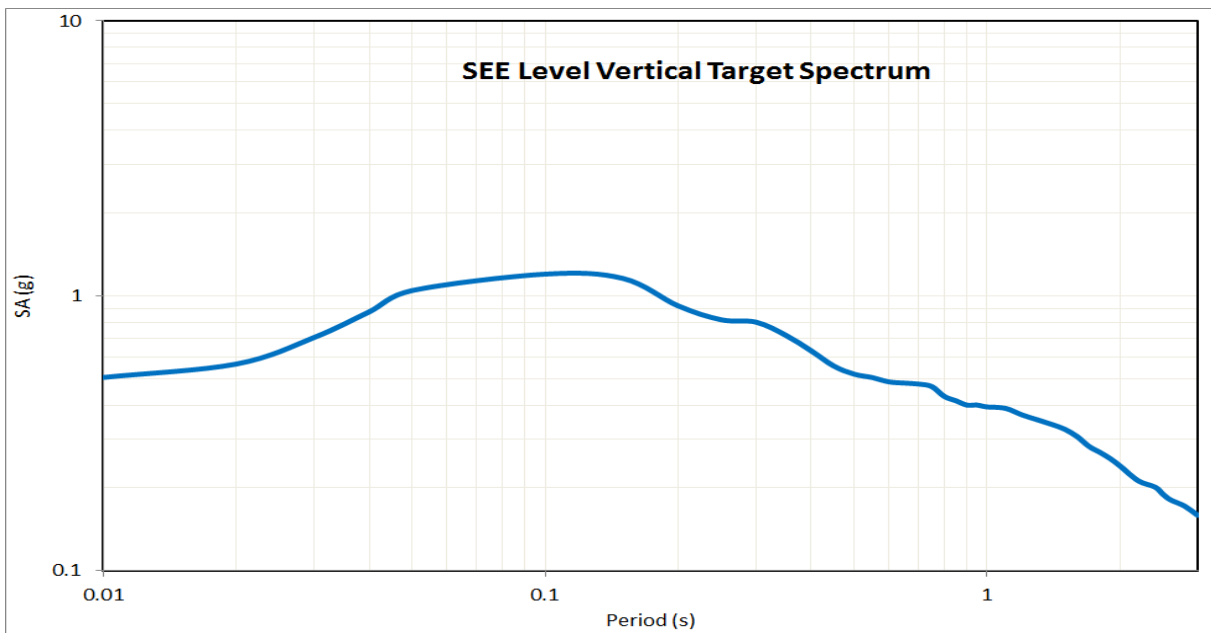


Figure 30. SEE level vertical response spectrum, obtained using coefficients after Bommer et.al, 2011).

13. CONCLUSIONS

A thorough analysis of the earthquake hazard at the Bisri Dam site is conducted to assess the following earthquake resistant design basis spectra:

The Operating Basis Earthquake is determined as the probabilistically assessed earthquake ground motion for an average return period of 144 years. The horizontal and vertical design basis spectra for the operating basis earthquake (OBE) for the random horizontal and vertical component are provided respectively in Figures 18 and 20. The response spectra is provided for 5% damping and for the free-field engineering bedrock outcrop. Under the action of this level of ground motion, the dam, appurtenant structures and equipment should remain functional and, if any, the minor damage should be easily repairable.

The Safety Evaluation Earthquake is determined to correspond to the 84-percentile deterministic MCE. The horizontal and vertical design basis spectra for the safety evaluation earthquake (SEE) for the random horizontal is are provided in Figure 25. Since the time domain analysis will be used for the SEE level design 7 sets of spectrum compatible scaled ground motion acceleration data are provided to enable the time-domain analysis. The vertical spectrum should be taken as the average of the vertical spectra of these sets of ground motion indicated in Figure 29. The 5% damped response spectra and the 7 sets of spectrum compatible scaled ground motion is provided is applicable at for the free-field engineering bedrock outcrop. Under the SEE the stability of the dam and life safety must be ensured with no uncontrolled release of water from the reservoir. SEE is the maximum level of ground motion for which the dam should be designed.

REFERENCES

Abrahamson, N. A. (2000). "Effects of rupture directivity on probabilistic seismic hazard analysis." Sixth International Conference on Seismic Zonation, Earthquake Engineering Research Inst., Oakland, California.

Abrahamson, N. and W. Silva (2008) "Summary of the Abrahamson & Silva NGA Ground-Motion Relations" Earthquake Spectra, Volume 24, No. 1, pp. 67–97.

Akkar, S. and Bommer, J.J. (2010). Empirical equations for the prediction of PGA, PGV and spectral accelerations in Europe, the Mediterranean region and the Middle East. Seismological Research Letters. 81:2, 195-206.

Akkar, S. and Cagnan, Z. (2010). A local ground-motion predictive model for Turkey and its comparison with other regional and global ground-motion models. Bulletin of the Seismological Society of America. 100:6, 2978-2995.

Akkar, S., Sandikkaya, M.A. and Bommer, J.J. (2014), "Empirical ground-motion models for point- and extended- source crustal earthquake scenarios in Europe and the Middle East" Bulletin of Earthquake Engineering, 12(1), 359-387.

Al-Tarazi, E. and E.Sandvol (2007), Alternative Models of Seismic Hazard Evaluation along the Jordan–Dead Sea Transform, Earthquake Spectra, Volume 23, No. 1, pages 1–19.

Ambraseys, N.N. (1997): The earthquake of 1 January 1837 in Southern Lebanon and Northern Israel, Ann. Geofis., XL (4), 923-935.

- Ambraseys, N.N. and C.P. Melville (1988): An analysis of the Eastern Mediterranean earthquake of 20 May 1202, in *History of Seismography and Earthquakes of the World*, edited by W.H. LEE (Academic, San Diego,CA), 181-200.
- Ambraseys, N.N. and M. Barazangi (1989): The 1759 earthquake in the Bekaa Valley: implications for earthquake hazard assessment in the Eastern Mediterranean region, *J. Geophys. Res.*, 94, 4007-4013.
- Ambraseys, N.N. and J.A. Jackson (1998): Faulting associated with historical and recent earthquakes in Eastern Mediterranean region, *Geophys. J. Int.*, 133, 390-406.
- Ambraseys, N.N., C.P. Melville and R.D. Adams (1994): *The Seismicity of Egypt, Arabia and the Red Sea: a Historical Review* (Cambridge University Press).
- ASCE 7-10 (2010), *Minimum Design Loads for Buildings and Other Structures*, ASCE Standard ASCE-SEI 7-10, American Society of Civil Engineers.
- Baker, J.W., Y. Bozorgnia, C. Di Alessandro, B.Chiou, M.Erdik, P. Somerville and W.Silva (2012), GEM- PEER Global GMPEs Project Guidance for Including Near-Fault Effects in Ground Motion Prediction Models, *Proc. 15th WCEE, Lisboa*
- Bard P-Y (2014), *Accelerograms for Preliminary Computations of the Stability of Bisri Dam: Selection of Accelerograms for Preliminary Computations of the Stability of the Bisri Dam (Lebanon) and Comments on the Underground Velocity Profile, March 2014*
- Bommer J, Douglas J, Scherbaum F., Cotton F, Bungum H, and Fäh D. (2010), On the selection of ground motion prediction equations for Sesimic Hazard Analysis, *Seismological Research Letters*; September/October 2010; v. 81; no. 5; p. 783-793; DOI: 10.1785/gssrl.81.5.783
- Bommer, J.J., S.Akkar and Ö. Kale (2011), A Model for Vertical-to-Horizontal Response Spectral Ratios for Europe and the Middle East, *Bulletin of the Seismological Society of America*, Vol. 101, No. 4, pp. 1783–1806
- Boore, D. M. and Atkinson, G. M., 2008. Ground-motion prediction equations for the average horizontal component of PGA, PGV, and 5%-damped PSA at spectral periods between 0.01s and 10.0 s, *Earthquake Spectra*, 24:1, 99–138.
- Butler, R.W.H. & Spencer, S. (1998). Structural evolution of a transform restraining bend - transpression on the Lebanese sector of the Dead Sea Fault System. In: *Continental transpressional and transtensional tectonics* (ed. R.E. Holdsworth , R.A. Strachan & J.F. Dewey) *Spec. Publ. Geol. Soc. London* 135, 81-106.
- Campbell, K. W. and Y. Bozorgnia (2008) “NGA Ground Motion Model for the Geometric Mean Horizontal Component of PGA, PGV, PGD and 5% Damped Linear Elastic Response Spectra for Periods Ranging from 0.01 to 10 s” *Earthquake Spectra*, Vol. 24, No. 1, pp: 139–171.
- Campbell, K.W. and Bozorgnia, Y. (2006). “Next generation attenuation (NGA) ground motion models: Can they be used in Europe?” *Proceedings of the 1st European Conference on Earthquake Engineering ad Seismology, Geneva, Switzerland, September 3-8, 2006, Paper 458.*
- Carton, H., Singh, S.C, Tapponnier, P., Elias, A., Briais, A., Sursock, A., Jomaa, R., King, G.C.P., Daëron, M., Jacques, E., Barrier, L (2009) “Seismic evidence for Neogene and active shortening offshore Lebanon (SHAUMAR cruise)”, *Journal of Geophysical Research* VOL. 114, B07407, doi:10.1029/2007JB005391.

- Cauzzi, C. and E. Faccioli (2008), Broadband (0.05 to 20s) prediction of displacement response spectra based on worldwide digital records. *Journal of Seismology*, 12(4):453–475, Oct 2008. doi: 10.1007/s10950-008-9098-y.
- Chiou, B.S.-J. and Youngs, R.R. (2008). An NGA model for the average horizontal component of peak ground motion and response spectra. *Earthquake Spectra*. 24:1, 173-215.
- Cotton, F., Scherbaum, F., Bommer, J.J. and Bungum, H. (2006). Criteria for Selecting and Adjusting Ground-Motion Models for Specific Target Regions: Application to Central Europe and Rock Sites. *Journal of Seismology*, 10, 137-156.
- Daeron, M., L. Benedetti, P. Tapponnier, A. Sursock, and R. Finkel (2004). Constraints on the post ~25-ka slip rate of the Yammouneh fault (Lebanon) using in situ cosmogenic ³⁶Cl dating of offset limestone-clast fans, *Earth Planet. Sci. Lett.* 227, 105–119.
- Daeron, M., Y. Klinger, P. Tapponnier, A. Elias, E. Jacques, and A. Sursock (2005), Sources of the large A.D. 1202 and 1759 Near East earthquakes, *Geology*, 33:7, 529– 532.
- Daeron, M. (2005) Role, cinématique et comportement sismique a long terme de la faille de Yammouneh, principale branche décrochante du coude transpressif libanais (faille du Levant), Institut de Physique du Globe a Paris.
- Daeron, M., Y. Klinger, P. Tapponnier, A. Elias, E. Jacques, and A. Sursock (2007), 12000-year-long record of 10 to 13 paleoearthquakes on the Yammouneh Fault, Levant Fault System, Lebanon, *Bull. Seismol. Soc. Am.*, 97:3, 749–771.
- Darawcheh, R., M.R. Sbeinati, C. Margottini and S. Paolini (2000): The 9 July 551 A.D. Beirut earthquake, Eastern Mediterranean region, *J. Earthquake Eng.*, 4, 403-414.
- Delavaud, E., Cotton, F., Akkar, S., Scherbaum, F., Danciu, L., Beauval, C., Drouet, S., Douglas, J., Basili, R., Sandikkaya, M.A., Segou, M., Faccioli, E. and Theodoulidis, N. (2012a). Toward a Ground-Motion Logic Tree for Probabilistic Seismic Hazard Assessment in Europe. *Journal of Seismology*, DOI: 10.1007/s10950- 012-9281-z.
- Delavaud, E., F. Cotton, C. Beauval, D.S. Akkar, F. Scherbaum and L. Danciu (2012b), Construction of a ground-motion logic tree for PSHA in Europe within the SHARE project, *Proc. 15th WCEE, Portugal*.
- Douglas J, Cotton, F., Di Alessandro, C., Boore, D.M., Abrahamson, N.A., and Akkar, S. (2012), Compilation and critical review of GMPEs for the GEM-PEER global GMPEs project, *Proc. 15th World Conf. Eqk. Eng.*, Lisbon, Portugal.
- Douglas, J. (2011), Ground motion prediction equations 1964-2010, Report PEER 2011/102, Pacific Earthquake Engineering Research Center, UC Berkeley, April.
- Dubertret, Louis (1955), Geological Map of Jezzine, Ministry of Public Works, Republic of Lebanon - Beirut.
- ECIDAH (1997), Bisri Dam: Updated Design Criteria for Final Design, Prepared by ECI and Dar Al Handasah Nazih Taleb & Partners.
- Elias, A. (2014), Report on the Neo-Tectonic Setting and Seismic Sources for the Seismic Hazard Assessment of the Bisri Dam Site, Neo-Tectonic Investigation of the Bisri Dam Site, August 2014.
- Elias, A. 2006. Le chevauchement de Tripoli-Saïda : croissance du Mont-Liban et risque sismique. Institut de Physique du Globe a Paris.

- Elias, A., Tapponnier, P., Singh, S.C., King, G.C.P., Briais, A., Daëron, M., Carton, H., Surssock, A., Jacques, E., Jomaa, R., and Klinger, Y. (2007) Active thrusting offshore Mount Lebanon: Source of the tsunamigenic A.D. 551 Beirut-Tripoli earthquake, *Geology*, 35:8, 755– 758.
- Ellsworth, W. L. (2003). Magnitude and area data for strike-slip earthquakes, U.S. Geol. Surv. Open-File Rept. 03-214 Appendix D.
- Elnashai, A. and R. El-Khoury (2004), *Earthquake Hazard in Lebanon*, Imperial College Press, London
- Erdik, M., K. Şeşetyan, M.B. Demircioğlu, C. Tüzün, D. Giardini, L.Gülen, D.S. Akkar, M. Zare (2012), Assessment of Seismic Hazard in the Middle East and Caucasus:EMME (Earthquake Model of Middle East) Project, Proc. 15th WCEE, Portugal.
- FEMA (2005). *Federal Guidelines for Dam Safety: Earthquake Analyses and Design of Dams*. NDSRB.
- Ferry, M., M. Meghraoui, N. Abou Karaki, M. Al-Taj, and L. Khalil (2011), Episodic Behavior of the Jordan Valley Section of the Dead Sea Fault, *Bulletin of the Seismological Society of America*, Vol. 101, No. 1, pp. 39–67, February 2011, doi: 10.1785/0120100097.
- Frankel AD, Mueller C, Barnhard T, Perkins D, Leyendecker E, Dickman N. S Hanson and M Hopper *National Seismic Hazard Maps: Documentation June*, USGS Open File Report 96- National seismic hazard maps: documentation June, USGS Open File Report 96–532.1996
- Girdler, R.W. (1990), The Dead Sea transform fault system. *Tectonophysics*, 180, 1-13.
- Gomez, F., Karam, G., Khawlie, M., McClusky, S., Vernant, P., Reilinger, R., Jaafar, R., Tabet, C., Khair, K., and Barazangi, M., 2007. Global Positioning System measurements of strain accumulation and slip transfer through the restraining bend along the Dead Sea fault system in Lebanon, *Geophysical Journal International*, 168, 1021-1028.
- Grünthal, G., C.Bosse, S.Sellami. D. Mayer-Rosa and D.Giardini (1999), *Compilation of the GSHAP Regional Seismic Hazard for Europe, Africa and the Middle East*, *Annali di Geofisica*, v.42, No.6.
- Gülerce, Z., and N. A. Abrahamson (2011). Site-specific spectra for vertical ground motion, *Earthq. Spectra*, 27, no. 4
- Hanks, T. C., and W. H. Bakun (2008), M-log A observations of recent large earthquakes, *Bull. Seismol. Soc. Am.* 98, 490.
- Hanks, T. C., and W. H. Bakun (2002), A bilinear source-scaling model for M-log A Observations of continental earthquakes, *Bull. Seismol. Soc. Amer.*, 92, 1841-1846.
- Huijjer, C., M. Harajli and S. Sadek (2011), Upgrading The Seismic Hazard of Lebanon in Light of the Recent Discovery of the Offshore Thrust Fault System, *Lebanese Science Journal*, Vol. 12, No. 2, 2011
- IAEA SSG-9 (2010) *Seismic Hazards in Site Evaluation for Nuclear Hazard, Specific Safety Guide*, No. SSG-9 International Atomic Energy Agency
- ICOLD (1989). *International Commission on Large Dams - Guidelines for selecting seismic parameters for large dams*. Paris.

- ICOLD (2010), Selecting seismic parameters for large dams. Guidelines, Revision of Bulletin 72, Committee on Seismic Aspects of Dam Design, International Commission on Large Dams, Paris.
- Idriss, M.I. (2008) “An NGA Empirical Model for Estimating the Horizontal Spectral Values Generated By Shallow Crustal Earthquakes” *Earthquake Spectra*, Vol. 24, No. 1, pp. 217–242.
- Kale, O. and Akkar, S. (2012). A novel procedure for selecting and ranking candidate ground-motion prediction equations (GMPEs) for seismic hazard analysis: Euclidean distance based ranking (EDR) method. *Bulletin of the Seismological Society of America*.
- Khair, K. (2001), Geomorphology and seismicity of the Roum fault as one of the active branches of the Dead Sea fault system in Lebanon, *J. Geophys. Res.*, 106(B3), 4233–4245.
- Nemer, T. and M. Meghraoui (2006) Evidence of coseismic ruptures along the Roum fault (Lebanon): a possible source for the AD 1837 earthquake *Journal of Structural Geology* 28, 1483-1495
- Nemer, T., M. Meghraoui, and K. Khair (2008). The Rachaya-Serghaya fault system (Lebanon): Evidence of coseismic ruptures, and the AD 1759 earthquake sequence, *J. Geophys. Res.* 113, no. B05312, doi 10.1029/2007JB005090.
- NIST (2011), Soil-Foundation-Structure Interaction for Building Structures, NIST GCR 11-917-15, prepared by the NEHRP Consultants Joint Venture for the National Institute of Standards and Technology, Gaithersburg, Maryland.
- Rowshandel, B. (2010). “Directivity Correction for the Next Generation Attenuation (NGA) Relations.” *Earthquake Spectra*, 26(2), 525-559.
- Sadek S and Harajli M. (2007) “Updated Seismic Hazard for Lebanon and Implications on Micro-Zonation” 4th International Conference on Earthquake Geotechnical Engineering, Thessaloniki-Greece, 25-28 June 2007.
- Sbeinati, M. R., R. Darawcheh, and M. Mouty (2005). The historical earthquakes of Syria: An analysis of large and moderate earthquakes from 1365 B.C. to 1900 A.D, *Ann. Geophys.* 48, 347–435.
- Scasserra, G., Stewart, J.P., Bazzurro, P., Lanzo, G., Mollaioli, F. (2009), A Comparison of NGA Ground-Motion Prediction Equations to Italian Data, *BSSA*, 99, 5, 2961-2978
- Seed, H.B., Ugas, C., and Lysmer, J. (1976), Site-Dependent Spectra for Earthquake-Resistant Design”, *BSSA*, 66, 1, 221-243.
- Shahi, S. K., and Baker, J. W. (2011). “An Empirically Calibrated Framework for Including the Effects of Near - Fault Directivity in Probabilistic Seismic Hazard Analysis.” *Bulletin of the Seismological Society of America*, 101(2), 742-755.
- Shapira, A. and R.Hofstetter (2007), Earthquake Hazard Assessments for Building Codes: Final Report, USAID Grant No:PCE-G-00-99-00038
- Shaw, B. E. (2009). Constant stress drop from small to great earthquakes in magnitude-area scaling, *Bull. Seismol. Soc. Am.* 99, 871,
- Somerville, P. G., Smith, N. F., Graves, R. W., and Abrahamson, N. A. (1997). “Modification of Empirical Strong Ground Motion Attenuation Relations to Include the Amplitude and Duration Effects of Rupture Directivity.” *Seismological Research Letters*, 68(1), 199-222.

- Spudich, P., and Chiou, B. S. J. (2008). "Directivity in NGA Earthquake Ground Motions: Analysis Using Isochrone Theory." *Earthquake Spectra*, 24(1), 279-298.
- Spudich, P., Chiou, B. S., Graves, R. W., Collins, K. R., and Somerville, P. G. (2004). A formulation of Directivity for earthquake sources using isochrone theory. 54.
- Spudich, P., Somerville, P. G., Shahi, S. K., Rowshandel, B., Chiou, B. S. J., Bayless, J., and Baker, J. W. (2012). "Directivity models produced for the Next Generation Attenuation West 2 (NGAW2) project." *Proceedings of 15th World Conference on Earthquake Engineering*, Lisbon, Portugal.
- Stafford, P.J., Strasser, F.O., and Bommer, J.J. (2008), "An evaluation of the applicability of the NGA models to ground-motion prediction in the Euro-Mediterranean region", *Bulletin of Earthquake Engineering*, Vol. 6, 149-177
- Stewart, J.P., J. Douglas, M. Javanbarg, Y. Bozorgnia, N.A. Abrahamson, D.M. Boore, K.W. Campbell, E. Delavaud, M.Erdik and P.J. Stafford (2014), Selection of Ground Motion Prediction Equations for the Global Earthquake Model, *Earthquake Spectra*.
- Strasser, F.O., M. C. Arango and J. J. Bommer (2010), Scaling of the Source Dimensions of Interface and Intraslab Subduction-zone Earthquakes with Moment Magnitude, *Seismological Research Letters* Volume 81, Number 6.
- USACE (1995). *Engineering Manual-Response Spectra and Seismic Analysis for Concrete Hydraulic Structures*, EC 1110-2-6050. Washington, D.C.: Chief of Engineers.
- USACE (2007). *Engineering and Design - Earthquake Design and Evaluation of Concrete Hydraulic Structures* EM 1110-2-6053. Washington, D.C.: Chief of Engineers.
- Wells & Coppersmith (1994) *New Empirical Relationships among Magnitude, Rupture Length, Rupture Width, Rupture Area, and Surface Displacement*. BSSA 84, 974-1002.
- Zare, M., H. Amini, P. Yazdi, K.Sesetyan, M. B. Demircioglu, D. Kalafat, M. Erdik, D. Giardini, M. A. Khan and N. Tsereteli (2014), Recent developments of the Middle East catalog, *J Seismol* (2014) 18:749–772.
- Zhao, J.X., Zhang, J., Asano, A., Ohno, Y., Oouchi, T., Takahashi, T., Ogawa, H., Irikura, K. Thio, H.K., Somerville, P.G. and Fukushima, Y. (2006). Attenuation relations of strong ground motion in Japan using site classification based on predominant period. *Bulletin of the Seismological Society of America*, 96:3, 898- 913.